

CHIANTI – an Atomic Database for Emission Lines

Paper VI: Proton Rates and Other Improvements

P. R. Young,^{1,2} G. Del Zanna,³ E. Landi,^{4,5} K. P. Dere,⁵ H. E. Mason,³
and
M. Landini⁶

ABSTRACT

The CHIANTI atomic database contains atomic energy levels, wavelengths, radiative transition probabilities and electron excitation data for a large number of ions of astrophysical interest. Version 4 has been released, and proton excitation data is now included, principally for ground configuration levels that are close in energy. The fitting procedure for excitation data, both electrons and protons, has been extended to allow 9 point spline fits in addition to the previous 5 point spline fits. This allows higher quality fits to data from close-coupling calculations where resonances can lead to significant structure in the Maxwellian-averaged collision strengths. The effects of photoexcitation and stimulated emission by a blackbody radiation field in a spherical geometry on the level balance equations of the CHIANTI ions can now be studied following modifications to the CHIANTI software. With the addition of H I, He I and N I, the first neutral species have been added to CHIANTI. Many updates to existing ion data-sets are described, while several new ions have been added to the database, including Ar IV, Fe VI and Ni XXI. The two-photon continuum is now included in the spectral synthesis routines, and a new code for calculating the relativistic free-free continuum has been added. The treatment of the free-bound continuum has also been updated.

Subject headings: atomic database – synthetic spectra – solar atmosphere – stellar atmosphere

¹Harvard-Smithsonian Center for Astrophysics, 60 Garden Street, Cambridge, MA 02138

²Present address: Space Science and Technology Department, Rutherford Appleton Laboratory, Chilton, Didcot, Oxfordshire OX11 0QX, U.K.

³Department of Applied Mathematics and Theoretical Physics, University of Cambridge, Silver Street, Cambridge CB3 9EW, UK

⁴ARTEP, Inc., Columbia, MD 21044

⁵Naval Research Laboratory, Washington DC, 20375

⁶Dipartimento di Astronomia e Scienza dello Spazio, Università di Firenze, Firenze, Italy

1. Introduction

The CHIANTI database was first released in 1996 (Dere et al. 1997) and it contains energy levels, radiative data and electron excitation rates for virtually all astrophysically important ions. In addition there are a number of computer routines written in IDL which allow a user to compute synthetic spectra and study plasma diagnostics. The database was originally focussed towards reproducing collisionally-excited emission line spectra at ultraviolet wavelengths from 50 to 1150 Å. Version 2 (Landi et al. 1999) introduced many minor ion species to the database as well as routines to compute free-free and free-bound continua. The most recent version (v.3) of the database (Dere et al. 2001) extended coverage of CHIANTI to X-ray wavelengths (1–50 Å) principally through the addition of hydrogen and helium-like ions, and dielectronic recombination lines.

CHIANTI has seen applications to many different areas of astrophysics since its inception. It has been extensively used in solar physics, in particular for the analysis of spectra obtained from the CDS, SUMER and UVCS spectrometers on board the SOHO satellite (e.g., Young & Mason 1997; Landi et al. 2002; Akmal et al. 2001). CHIANTI is also used to model the instrument responses of the EIT (Dere et al. 2000) and TRACE imaging instruments in order to convert measured fluxes into physical parameters such as temperature and emission measure. The wide coverage of many different ions allowed CHIANTI to be a useful aid in the verification and definition of ultraviolet spectrometers' flux calibrations through the use of emission line ratios that are insensitive to the plasma conditions. Examples include the SERTS rocket flights (Young et al. 1998; Brosius et al. 1998), and the Normal Incidence Spectrometer and Grazing Incidence Spectrometers on CDS (Del Zanna et al. 2001).

Beyond the Sun, CHIANTI has seen application to analyses of the wind emission from the Arches cluster of massive stars (Raga et al. 2001), warm gas in galaxy clusters (Dixon et al. 2001) and analyses of a number of cool stars including AB Doradus (Brandt et al. 2001), AU Microscopii (Pagano et al. 2000) and ϵ Eridani (Jordan et al. 2001). Del Zanna et al. (2002) present a review of various spectroscopic diagnostic techniques that can be applied to XUV observations of active stars. They use CHIANTI to illustrate the severe limitations that some commonly-used methods and atomic data have. Del Zanna et al. (2002) obtain results in terms of stellar transition region densities, emission measures and elemental abundances that are significantly different from those of other authors. Their results suggest that a large body of work on cool star atmospheres will have to be revisited and stress the importance of using assessed and up-to-date atomic data. Laboratory work also plays a vital role in the assessment of cool star results, with work by Beiersdorfer et al. (1999), Brown et al. (1998) and Fournier et al. (2001) providing valuable insights into plasma processes affecting EUV and X-ray spectra.

CHIANTI also forms a significant part of other atomic database packages. APED (Smith et al. 2001) supplements CHIANTI with data from several other sources and is focussed towards modeling X-ray spectra. XSTAR (Bautista & Kallman 2001) is a photoionization code that uses CHIANTI data for modelling the level balance within individual ions. CHIANTI also forms a significant part

of the Arcetri Spectral Code (Landi & Landini 1998, 2002).

The present work describes the latest updates to CHIANTI, including the addition of the new physical processes of proton and photon excitation of ion levels, the addition of new ions and revisions of existing ion data-sets.

2. Level balance equations

In version 4 of CHIANTI extra processes are now included in the level balance equations for ions, namely proton excitation and de-excitation, photoexcitation and stimulated emission. The level balance equations are

$$n_i \sum_{j \neq i} \alpha_{ij} = \sum_{j \neq i} n_j \alpha_{ji} \quad (1)$$

where i and j are indices for the individual levels within an ion, n_i is the population of level i relative to the population of ions as a whole, and α_{ij} is the number of i to j transitions taking place per unit time. In previous versions of CHIANTI, the α_{ij} were of the form

$$\alpha_{ij} = N_e C_{ij} + A_{ij} \quad (2)$$

where A_{ij} is the radiative decay rate (zero if $i < j$) and C_{ij} is the electron rate coefficient such that

$$C_{ij} = \frac{\omega_j}{\omega_i} \exp\left(-\frac{\Delta E}{kT}\right) C_{ji} \quad i < j \quad (3)$$

where C_{ij} is defined in Eq. 5 of Dere et al. (1997), ω_i is the statistical weight of level i , ΔE is the positive energy separation of levels i and j , k is the Boltzmann constant and T the electron temperature.

For version 4, α now takes the form

$$\alpha_{ij} = N_e C_{ij} + N_p C_{ij}^p + \mathcal{A}_{ij} \quad (4)$$

where N_p is the proton number density, C_{ij}^p is the proton rate coefficient, and \mathcal{A}_{ij} is the generalized radiative transition rate.

2.1. Proton rates

The inclusion of proton rates in ion level balance equations was first demonstrated to be important in solar coronal conditions by Seaton (1964) for the Fe XIV ion. He showed that the proton rates can become comparable to the electron excitation rates for transitions for which $\Delta E \ll kT$. Typically only transitions within the ground configuration of an ion are important and so, compared to the electron processes, relatively little data are required to account for proton processes in a particular ion. Whereas electron collision data are usually published in the form of collision strengths or Maxwellian-averaged collision strengths, proton collision data are generally published directly as rate coefficients. As positively-charged ions repel protons, the rate coefficient falls to zero at the threshold energy for the transition, and so tabulated values of rate coefficients typically change by several orders of magnitude over a small temperature range. Examples are shown in Fig. 1 from Ne VI (boron-like) and Fe XVIII (fluorine-like), where the proton rate coefficients are plotted for the ground transitions of these ions. Also shown for comparison are the electron rate coefficients for these transitions, derived from the data in CHIANTI. The proton rates are seen to be comparable in strength to the electron rates at the temperature of maximum ionization, T_{\max} of the ions, and become stronger at higher temperatures. We note, however, that the populations of the upper levels of ground configuration transitions are often dominated by cascading from higher levels in the ion rather than direct excitation (Mason 1975).

Examples of how proton rates can affect key diagnostic emission lines are demonstrated in Fig. 2. The Fe XVIII $\lambda 974$ line is prominent in flaring, solar plasma (Doschek et al. 1975) and has been recently been observed in a spectrum of the star Capella (Young et al. 2001). The Fe XXI $\lambda 102/\lambda 128$ ratio is a key density diagnostic for solar flares (Mason et al. 1979) and active stars (Dupree et al. 1993).

2.2. Implementation of proton rates in CHIANTI

For each ion for which proton rates are available, an additional file is required in the database to contain the fits to the rate coefficients. The file has the suffix .PSPLUPS, and is exactly analogous to the .SPLUPS file for the electron fits. All of the proton transitions included in CHIANTI are forbidden transitions taking place between levels within the same configuration, and so they are treated as Type 2 in the Burgess & Tully (1992) formalism. Many of the transitions required 9-point splines (see Sect. 3) in order to provide adequate fits. The 9-point splines can only be applied when there are at least 9 points to be fitted. For some transitions with less than 9 data points, the 5 point spline fit applied to Type 2 transitions could not adequately fit the data. In these cases a new fit type, Type 6, was introduced whose scaling is as follows

$$x = \frac{\left(\frac{kT}{\Delta E}\right)}{\left(\frac{kT}{\Delta E} + a\right)} \quad (5)$$

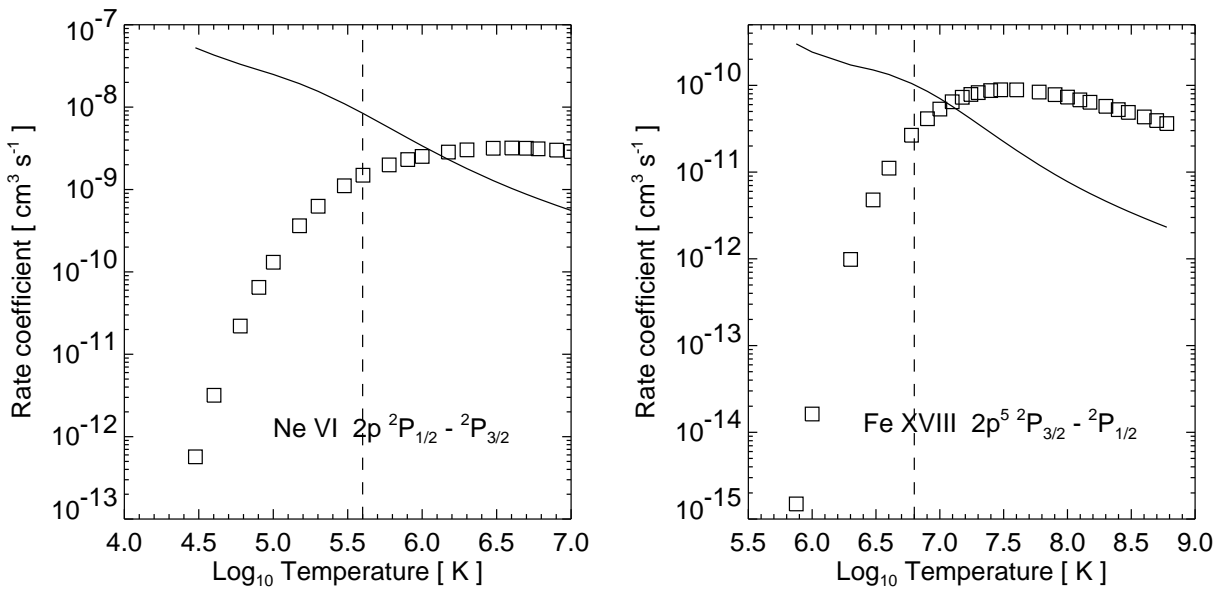


Fig. 1.— Proton rate coefficients (squares) for the ground transitions of (a) Ne VI (Foster et al. 1997) and (b) Fe XVIII (Foster et al. 1994b), demonstrating the sharp fall at low temperatures due to the collision strengths falling to zero at the threshold energy. For comparison, the electron rate coefficients derived from CHIANTI are plotted as continuous curves. The dashed, vertical lines show the T_{\max} of the ions.

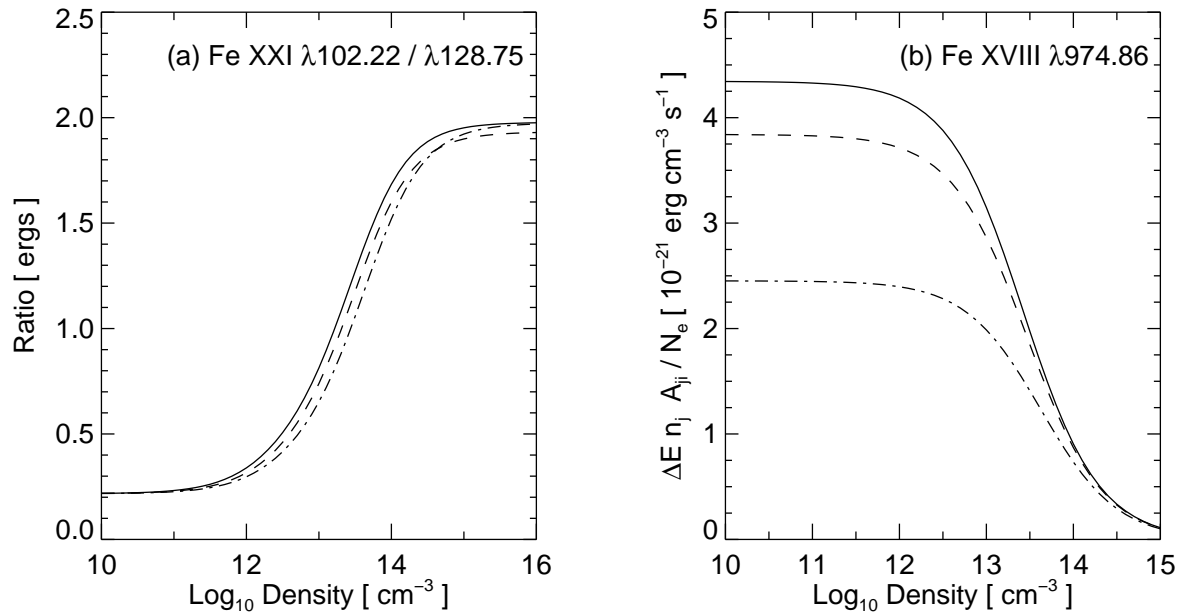


Fig. 2.— Plot (a) compares the Fe XXI $\lambda 102.22 / \lambda 128.75$ density diagnostic in the cases when proton rates are included (solid line) and when they are not included (dashed line). Also plotted is the ratio from the previous version of the CHIANTI database (dash-dot line). Plot (b) provides a similar comparison but for the Fe XVIII $\lambda 974.86$ line emissivity. In both cases the addition of proton rates and the update of the electron excitation rate result in significant differences.

$$y = \log C_{ij}^p \quad (6)$$

where a is the scaling parameter. By taking the logarithm of the rate coefficient, the steep gradients in the rate coefficient could be overcome and reasonable 5-point spline fits obtained. As errors in the fit are amplified when fitting logarithm data, care was taken to ensure that the rate coefficients derived from the fits were $\lesssim 1\%$ from the original data values.

For some ions the only rate coefficient data available had been calculated at a single temperature. These data were incorporated into CHIANTI by assuming a Type 2 transition and setting the five points of the spline to lie on a straight line. The gradient of the line was set such that $y = 0$ at $x = 0$, and $y = C_{ij}^p$ at $x = 0.90$. This method ensures that the rate coefficients derived from the spline fall sharply to zero at low temperatures, and that at high temperatures the rates tend to a constant value that is around 10% higher than the original data value.

The number density of protons, N_p , is required in Eq. 4 and it is calculated from the ion balance and element abundance files contained in CHIANTI through the following expression

$$R(T) = \frac{N_p}{N_e} = \frac{\text{Ab}(\text{H}) F(\text{H}^+, T)}{\sum_{i=1}^n \sum_{Z=1}^i Z F(\text{A}_i^{+Z}, T) \text{Ab}(\text{A}_i)} \quad (7)$$

where Ab is the element abundance, A_i is the i th element (i.e., $\text{A}_1 = \text{H}$, $\text{A}_2 = \text{He}$, etc.), Z is the charge on the ion, and $F(\text{A}_i^{+Z}, T)$ is the fraction of ions of element A_i in the form A_i^{+Z} at temperature T .

The ion fractions contained in CHIANTI are tabulated over the range $4.0 \leq \log T \leq 8.0$. Above and below these values, we set $R(T)$ to the values for $\log T = 8.0$ and $\log T = 4.0$, respectively. The default ion balance file used in calculating $R(T)$ is Mazzotta et al. (1998), while the default abundances are the solar photospheric values of Grevesse & Sauval (1998).

2.3. Photoexcitation and Stimulated Emission

The generalized photon rate coefficient in the presence of a blackbody radiation field of temperature T_* is given by

$$\mathcal{A}_{ij} = \begin{cases} W(R) A_{ji} \frac{\omega_j}{\omega_i} \frac{1}{\exp(\Delta E/kT_*) - 1} & i < j \\ A_{ij} \left[1 + W(R) \frac{1}{\exp(\Delta E/kT_*) - 1} \right] & i > j \end{cases} \quad (8)$$

where A_{ji} is the radiative decay rate and $W(R)$ is the radiation dilution factor which accounts for the weakening of the radiation field at distances R from the source center. For a uniform (no limb brightening/darkening) spherical source with radius R_*

$$W = \frac{1}{2} \left[1 - \left(1 - \frac{1}{r^2} \right)^{1/2} \right] \quad (9)$$

where

$$r = \frac{R}{R_*} \quad (10)$$

2.4. Implementation of Photoexcitation and Stimulated Emission in CHIANTI

No additions or modifications to CHIANTI data files are required for photoexcitation and stimulated emission as their rates are entirely determined from the radiative decay rates, level separation energies, and statistical weights – information already contained in CHIANTI. It is only necessary to specify the radiation field temperature and the dilution factor, which are done through inputs to the IDL procedures with the new keywords RPHOT and RADTEMP. RPHOT specifies r , the distance from the center of the radiation source in source radii units, while RADTEMP gives the blackbody radiation temperature in K. By default, photoexcitation and stimulated emission are not included in the level balance equations unless the keywords are set.

It is important to remember the assumptions in our formalism for radiation processes. For a given ion, only very specific wavelengths in the radiation continuum will affect the ion's level balance. If there are significant deviations from a blackbody spectrum at any of these wavelengths (perhaps due to a deep absorption line) then CHIANTI may not model the ion entirely correctly.

Examples of specific uses of the extra radiation processes include modeling of coronal emission lines above the surface of the Sun and other cool stars when the coronal electron density falls to low enough values that electron collisions lose their potency. Fig. 3 shows the Fe XIII $\lambda 10746/\lambda 10797$ ratio as a function of density, calculated in the cases of there being no radiation field ($W = 0$) and when the Fe XIII ions are located 0.1 source radii ($W = 0.29$) above the surface of a 6000 K blackbody, typical of the Sun. The Fe XIII infrared lines are an important density diagnostic for ground-based solar coronal studies (e.g., Penn et al. 1994), and are potential probes of the solar coronal magnetic field (Judge 1998). Photoexcitation can also be important for modeling nebular ions that are irradiated by a hot star, such as in planetary nebulae, symbiotic stars and Wolf-Rayet stars.

3. 9-point spline fitting

Increasingly, the electron excitation data supplied by atomic physicists are performed in the R -matrix approximation which leads to extremely complex structure in the calculated collision

strengths, Ω . These data are provided in a more convenient form as Maxwellian-averaged collision strengths, Υ , that are a comparatively smooth function of temperature, and suitable for fitting with the 5-point splines employed in the previous versions of the CHIANTI database. However, in some cases, it was necessary to restrict the range of the original data in order to improve the fit for temperatures of usefulness to astrophysical conditions. An example is shown in Fig. 4 where one can see that at high and low temperatures (well away from the temperature of maximum ionization, T_{\max} , of the ion) the Υ values derived from the CHIANTI fit deviate significantly from the original data values. An accurate fit to both the low and high temperature data points would require a spline with a larger number of node points. For all of the ions included up to and including v.3 of CHIANTI where the temperature range of the original Υ data has been restricted, we have aimed to fit within 1% those data points within at least 1.0 dex of the $\log T_{\max}$ of the ion. This is adequate for all conditions likely to be met in stellar transition regions and coronae.

For some situations in astrophysics, particularly photoionized plasmas, ions can be formed at electron temperatures much lower than T_{\max} , in which case it is important to ensure accuracy of the CHIANTI fits at lower temperatures. We thus now allow 9-point spline fits to the data. In addition, the inclusion of proton rate coefficients into CHIANTI – described in the preceding section – requires 9-point spline fits on account of the wide range of variation of the rate coefficient with temperature.

The modifications made to the database and the accompanying IDL routines in order to deal with the 9-point spline fits are described in detail in a software note available from the CHIANTI web-page at <http://wwwsolar.nrl.navy.mil/chianti.html>. No new CHIANTI files are required; the 9-point spline fit data are incorporated into the .SPLUPS files.

4. The proton rate data

Several different methods have been employed by atomic physicists in deriving proton rate coefficients, and are reviewed in Dalgarno (1983) and Reid (1988). The most basic is the semiclassical (or impact-parameter) approach in which the position of the proton relative to the ion is treated classically and first order approximations are made for the interaction with the nucleus. This approximation was originally applied to Coulomb excitation of nuclei (Alder et al. 1956) and first extended to the proton excitation of ions by Seaton (1964). While the first order approximation is good for low energy collisions, at intermediate energies and low impact parameter values the first order approximation fails, and it is necessary to adopt a different approximation or solve numerically the coupled differential equations describing the interaction. Potentially the most accurate method is to treat the proton’s trajectory quantum mechanically and solve the complete set of close-coupling equations. Such an approach is commonly used in R -matrix calculations of electron collision cross-sections, however, it is computationally much more demanding for proton collisions. Within the semiclassical approach, it has been shown that symmetrizing the problem with respect to the initial and final velocities (Alder et al. 1956), and including polarization effects (Heil et al.

1982, 1983) can improve the accuracy of the proton cross-sections.

Specific methods that have yielded the data outlined in the following sections are as follows. Bely & Faucher (1970) used a symmetrized first order semiclassical approximation to calculating the proton cross-sections, and provided rate coefficients for a large number of ions with configurations $2p$, $2p^5$, $3p$ and $3p^5$. In the intermediate energy range where first order theory breaks down they employ an approximation referred to as Coulomb-Bethe II, borrowed from the theory of electron excitation of positive ions, to determine the cross-section.

Kastner & Bhatia (1979) (see also Kastner 1977) also used the first order semiclassical approximation for low energies while for intermediate energies a form for the cross section due to Bahcall & Wolff (1968) was used. At high energies a further approximation to the cross-section was suggested by Kastner & Bhatia (1979), and the combined cross-section yielded the rate coefficients. The advantage of this method is that it can be applied in a straightforward manner to a wide range of ions.

Landman (1973) developed a symmetrized, semiclassical close-coupling method to compute proton rates for Fe XIII. This method retains the classical treatment for the proton trajectory, but the transition probabilities are determined by numerically solving the close-coupling equations, removing the uncertainties at intermediate energies of the first order approximation. Landman's work was extended to a number of other ions in later papers (Landman 1975, 1978, 1980; Landman & Brown 1979).

P. Faucher used a fully quantal close-coupling method to compute proton cross-sections for a number of ions (Faucher 1975, 1977; Faucher et al. 1980). In Faucher & Landman (1977) the two authors compared their methods for computing proton rates, and found excellent agreement, demonstrating that the semiclassical approach is a good approximation for highly-ionized ions at typical astrophysical energies.

A number of papers by V.J. Foster, R.S.I. Ryans and co-workers have made use of the method of Reid & Schwarz (1969) to calculate proton rate coefficients for a large number of ions. A symmetrized, semiclassical close-coupling approximation is used, with polarization effects included.

Sources for most of the proton rate data assessed for CHIANTI were obtained from the review of Copeland et al. (1997), who give accuracy ratings for each of the calculations. We have selected for each ion those data-sets that have the highest accuracy ratings and that cover the widest temperature range. A number of new calculations have been published by V.J. Foster, R.S.I. Ryans and co-workers since this review and have been used where available. Ions in the hydrogen, helium, neon, sodium, argon and potassium iso-electronic sequences all have a single level in the ground configuration, and so proton rates play no role in the level balance of the ions. Consequently these sequences are not listed below. Fig. 5 summarizes which of the major elements' ions we have proton data for. Additional data is also available for some of the minor elements (Na, P, Mn, etc.) and these are discussed in the following sections.

4.1. Beryllium sequence

Rate coefficients for the $2s2p\ ^3P_J-^3P_{J'}$ transitions have been calculated by Ryans et al. (1998) using the method of Reid & Schwarz (1969) for the ions C III, N IV, O V, Ne VII, Mg IX, Al X, Si XI, S XIII, Ar XV, Ca XVII, Ti XIX, Cr XXI, Fe XXIII and Ni XXV. The rates were tabulated at 20 values of temperature spanning typically 2–3 orders of magnitude around the T_{\max} of the ions. All of the data were fit with 9 point splines. In some cases it was necessary to omit points at low and/or high temperatures in order to obtain a good fit.

4.2. Boron sequence

Foster et al. (1997) provided rate coefficients for the ground $2s^22p\ ^2P_{1/2}-^2P_{3/2}$ transition and the three $2s2p^2\ ^4P_J-^4P_{J'}$ transitions, tabulated for 20 temperatures spanning at least two orders of magnitude. While the $^2P_{1/2}-^2P_{3/2}$ data cover the temperature region ± 1 dex around the $\log T_{\max}$ of the ions, the data for the $^4P_J-^4P_{J'}$ transitions cover a lower temperature range and generally do not extend to 1 dex beyond the $\log T_{\max}$ of the ions. Thus care must be taken if such data are used at temperatures well beyond the T_{\max} of the ion.

Data for C II, N III, O IV, Ne VI, Mg VIII, Al IX, Si X, S XII, Ar XIV, Ca XVI, Ti XVIII, Cr XX, Mn XXI, Fe XXII and Ni XXIV have been added to CHIANTI and 9 point spline fits have been performed. For some of the transitions it was necessary to remove from the fit points at the beginning or end of the temperature range in order to improve the fit quality. The cross-sections were calculated with the method of Reid & Schwarz (1969).

4.3. Carbon sequence

Rate coefficients for the $2s^22p^2\ ^3P_J-^3P_{J'}$ transitions have been calculated by Ryans et al. (1999a, see also Ryans et al. 1999b) for the ions N II, O III, Ne V, Mg VII, Si IX, S XI, Ar XIII, Ca XV, Ti XVII, Cr XIX, Fe XXI and Ni XXIII. The method employed by Ryans et al. (1999a) is that of Reid & Schwarz (1969). Rates are tabulated for 20 temperatures spanning 2–3 orders of magnitude around the temperature of maximum ionization of the ions. All of the data were fit with 9 point splines. In some cases it was necessary to omit points at low and/or high temperatures in order to obtain a good fit.

The inclusion of proton rates is particularly important for the heavier ions in the carbon sequence. Fig. 2a demonstrates the effects for the Fe XXI $\lambda 102/\lambda 128$ density diagnostic ratio.

4.4. Nitrogen sequence

Proton rates are only available for a limited number of nitrogen-like ions. For Ti XVI we use the rates of Bhatia et al. (1980), calculated for nine transitions amongst the levels of the $2s^22p^3$ configuration at a temperature of 6.5×10^6 K. Feldman et al. (1980) give rates for Cr XVIII and Ni XXII for seven transitions amongst the levels of the $2s^22p^3$ configuration at temperatures of 7×10^6 K (Cr XVIII) and 1.1×10^7 K (Ni XXII). For each of Ti XVI, Cr XVIII and Ni XXII the method of Kastner & Bhatia (1979) was used to calculate the proton cross-sections.

Proton rates for Fe XX have been calculated by Bhatia & Mason (1980a) using the method of Bely & Faucher (1970) for all transitions amongst the levels of the ground configuration, tabulated at four temperatures between 6×10^6 K and 1.5×10^7 K.

For Si VIII the rates of Bhatia & Landi (2002a) have been incorporated. These are tabulated for all transitions in the ground configuration for nine temperatures over the range $5.6 \leq \log T \leq 6.4$. Bhatia & Young (1998) have calculated rates for eight transitions in the ground configuration of Mg VI at a single temperature of $\log T = 5.6$. The four transitions from the ground 4S level are very weak and have not been included in CHIANTI. For both Mg VI and Si VIII, the method of Kastner & Bhatia (1979) was used to calculate the proton cross-sections.

4.5. Oxygen sequence

Unpublished data of R.S.I. Ryans and co-workers (R.K. Smith 1999, private communication) for the $2s^22p^4$ 3P_J – $^3P_J'$ transitions of several oxygen-like ions have been fitted for CHIANTI. The ions are Ne III, Mg V, Si VII, S IX, Ar XI, Ca XIII, Ti XV, Cr XVII and Fe XIX. The proton rates are tabulated for 20 temperatures typically spanning two orders of magnitude around the T_{\max} of the ion. The cross-sections were calculated with the method of Reid & Schwarz (1969).

For the additional ions Na IV, Al VI and P VIII the data of Landman (1980) are used. The proton rates are tabulated for nine temperatures spanning a temperature interval of $\log T = 0.8$ around the T_{\max} of the ions, and were calculated with the method of Landman (1973). Typos in the tabulation of the proton rates for the 3P_1 – 3P_0 transitions in Na IV and Al VI at $\log T = 5.6$ have been corrected.

Rate coefficients for Ni XXI have been published by Feldman et al. (1980) for seven transitions amongst the levels of the ground configuration, calculated at a temperature of 10^7 K using the method of Kastner & Bhatia (1979). These single temperature data have been fit as described in Sect. 2.2 and added to CHIANTI.

4.6. Fluorine sequence

Proton rates for the $2s^22p^5 \ ^2P_{3/2}-^2P_{1/2}$ transition of four F-like ions have been taken from Foster et al. (1994a). The ions are Ne II, S VIII, Ti XIV, and Ni XX. The data are tabulated for 17 temperatures spanning temperature ranges of ≈ 1.5 dex around the T_{\max} of the ions, and were calculated using the method of Reid & Schwarz (1969).

Fe XVIII was treated separately by Foster et al. (1994b) who tabulated rates for 26 temperatures from 7.5×10^5 K to 6×10^8 K, again calculated with the method of Reid & Schwarz (1969). To obtain a good fit to this data, the two lowest and four highest temperatures points had to be omitted.

Data for eight further F-like ions – Na III, Mg IV, Al V, Si VI, P VII, Ar X, Ca XII and Cr XVI – have been published by Bely & Faucher (1970). The data are tabulated for 13 temperatures spanning more than an order of magnitude around the T_{\max} of the ions, and have been added to CHIANTI.

An example of how the addition of proton rates affects the Fe XVIII is presented in Fig. 2b where the emissivity of the $2s^22p^5 \ ^2P_{3/2}-^2P_{1/2}$ ground transition at 974.86 Å is increased by around 10%.

4.7. Magnesium sequence

Proton rate coefficients for the $^3P_J-^3P_{J'}$ transitions in the $3s3p$ excited configuration of Si III, S V, Ar VII, Ca IX and Fe XV have been fitted and added to CHIANTI. The rates were calculated by Landman & Brown (1979) and are tabulated for 11–13 temperatures at 0.1 dex intervals around the T_{\max} of the ions. The method for calculating the cross-sections is that of Landman (1973).

4.8. Aluminium sequence

Proton rates are only necessary for the $3s^23p \ ^2P_{1/2}-^2P_{3/2}$ transition in Al-like ions. J. Tully (private communication, 2001) has calculated rate coefficients for Fe XIV at 21 temperatures over the range $6.0 \leq \log T \leq 8.0$ and these are included in CHIANTI. The data cover a much broader temperature range than those of Heil et al. (1983), the data recommended by Copeland et al. (1997). Agreement is excellent at 1×10^6 K, but the two data-sets diverge at higher temperatures, with the Tully values being larger. This is likely due to Heil et al. (1983) only calculating the cross-section to energies ~ 900 eV which are not large enough to obtain reliable rate coefficients at high temperatures.

Data for a large number of Al-like ions are given in Bely & Faucher (1970), however, most of these ions are not included in CHIANTI and so we take data only for Si II, S IV and Ni XVI. The

rate coefficients are tabulated for 13 temperatures around the T_{\max} of the ions.

4.9. Silicon sequence

Only data for Fe XIII and Ni XV are available in the literature. For Fe XIII we use the proton rates of Landman (1975) that are tabulated for five temperatures between 1×10^6 and 3×10^6 K. Landman (1975) gives data for all transitions between the individual magnetic sub-levels of the $^3P_{0,1,2}$, 1D_2 and 1S_0 levels of the ground configuration. These rates have been summed according to Landman's Eq. 8.

Rates for Ni XV are presented in Faucher (1977) for transitions amongst the ground 3P levels. Data are given for nine temperatures between 5×10^5 K and 4.5×10^6 K. The method of calculation of the proton cross-sections is that of Faucher (1975).

4.10. Phosphorus sequence

Only data for Fe XII are available on the phosphorus isoelectronic sequence. Landman (1978) provided rate coefficients for all transitions within the ground $3s^23p^3$ configuration of Fe XII, tabulated at four temperatures between 1×10^6 K and 2.5×10^6 K and these are included in CHIANTI.

4.11. Sulphur sequence

Landman (1980) give proton rates for several members of the sulphur sequence, but only Fe XI and Ni XIII are contained in CHIANTI. For Fe XI Landman (1980) gives rates for transitions amongst the $3s^23p^4$ 3P_J ground levels, while for Ni XIII transitions from the 3P_2 and 3P_1 levels to all of the ground configuration levels are tabulated.

4.12. Chlorine sequence

For Fe X and Ni XII we use rate coefficients for the $3s^23p^5$ $^2P_{1/2}-^2P_{3/2}$ transition from Bely & Faucher (1970) who computed data at 13 temperatures over the ranges $5.2 \leq \log T \leq 6.5$ (Fe X) and $5.4 \leq \log T \leq 6.7$ (Ni XII). Bely & Faucher (1970) also give data for a number of other Cl-like ions, however they can not be included as no model exists for these ions as of version 4 of CHIANTI.

Data for additional transitions in Fe X were published by Bhatia & Doschek (1995) who gave rates at a single temperature of 1×10^6 K for 10 transitions from the $3s^23p^43d$ 4D levels. These single temperature data have been fit according to the method described in Sect. 2.2 and added to

CHIANTI. The method used to calculate the cross-sections is that of Kastner & Bhatia (1979).

5. New data for the standard database

The following sections describe new electron excitation, radiative and energy level data that have been added to CHIANTI since version 3. Table 1 summarizes which ions have been added or updated.

5.1. Hydrogen isoelectronic sequence

5.1.1. $H\,I$

The atomic model for H I includes the 25 fine structure levels of the $1s$, $2l$, $3l$, $4l$ and $5l$ configurations. Observed energies are taken from the National Institute of Science and Technology (NIST) Atomic Spectra Database (Fuhr et al. 1999). For oscillator strengths and radiative decay rates (A values) of allowed lines, the values of Wiese, Smith & Glennon (1966) have been used. The magnetic dipole and two photon decay rates from the first excited level $2s\ ^2S_{1/2}$ are taken from Parpia & Johnson (1982).

Maxwellian-averaged collision strengths are taken from the R -matrix calculations of Anderson et al. (2002) who consider the 15 LS levels up to $5l$. The orginal calculations of Anderson et al. (2000) had been assessed for inclusion in CHIANTI but it was found that their scaled collision strengths for allowed transitions did not approach the high temperature limit specified by Burgess & Tully (1992). This was brought to the attention of the authors who found an error in their treatment of the R -matrix calculations at high energies. Anderson et al. (2002) report the revised collision strengths. Fine structure collision strengths are derived under the assumption of LS coupling. Aggarwal et al. (1991) previously calculated H I collision strengths, also using R -matrix methods, but at lower energies and temperature than the Anderson calculations. In general, the two sets of calculations are in reasonable agreement at temperatures near 10^4 K but then tend to diverge at higher temperatures where differences on the order of a factor of 2 can often be found.

5.2. Helium isoelectronic sequence

5.2.1. $He\,I$

For the helium isoelectronic sequence, the 49 fine structure levels of the $1snl$ configurations, $n=1-5$ and $l = s, p, d, f, g$ are included. Observed energies are taken from the NIST Atomic Spectra Database (Fuhr et al. 1999). For oscillator strengths and radiative decay rates (A values) of allowed lines, the values of Wiese, Smith & Glennon (1966) have been used. The magnetic dipole transition

Ion	I	II	III	IV	V	VI	VII	VIII	IX	X	XI	XII	XIII	XIV	XV	XVI
H	*															
He	*	o														
C	o	o	•	o	o											
N	*	o	o	o	o	o	o									
O	•	o	o	•	•	o	o									
Ne	o	•	o	•	o	o	o	o	o	o						
Na	o	o	o	o	o	o	o	o	o	o						
Mg	o	o	o	•	o	o	o	o	o	o						
Al	o	o	o	o	•	o	•	•	o	o			o			
Si	o	o	o	o	o	•	o	•	•	o			o			
P		o		o	o	•	o	o	o	o			o			
S	•	o	o	o	o	o	•	•	o	•	•	o	o	o		
Cl													o			
Ar		*					o	o	o	o	•	o	•	•	o	
K							o	o	o	o	•	o	o	o	o	
Ca							o	o	o	o	o	o	•	o	•	
Ti								o	o			o	o	o	•	
Cr									o	o			o	o		o
Mn									o							o
Fe	o			*	o	o	o	o	o	•	o	o	o	•	o	
Co																
Ni									o	o		o	o	o	o	
Zn																

Ion	XVII	XVIII	XIX	XX	XXI	XXII	XXIII	XXIV	XXV	XXVI	XXVII	XXVIII
Ar	o	o										
K	o											
Ca	•	o	o	o								
Ti	o	o	o	o								
Cr	o	•	o	o	o	o	o					
Mn	o	o	•	o	o	o	o	o				
Fe	o	•	•	•	•	•	•	•	o	o		
Co	o		o	•	o	o	o	o	o			
Ni	o	o	o	o	*	•	o	o	o	o	o	o
Zn			o				•	o	o	o	o	o

Table 1: Ions included in the CHIANTI database. o: Ions in the CHIANTI 3.0 version *not* changed in the present update. •: Ions in the CHIANTI 3.0 version whose data have been modified/complemented in the present update. *: New entries for the CHIANTI version 4.0 database.

probabilities for $1s\ 1S_0 - 2s\ 3S_1$, $1s\ 1S_0 - 2p\ 3P_{1,2}$ and $2s\ 3S_1 - 2p\ 3P_{0,1,2}$ are taken from the calculations of Lin et al. (1977). The two photon decay rate for $1s\ 1S_0 - 2s\ 1S_0$ is taken from Drake (1986).

Sawey & Berrington (1993) have calculated collision strengths for He I for all of the levels included in the current CHIANTI model. Maxwellian-averaged collision strengths between temperatures of 2000 and 30,000 K are provided. Since the population of He I peaks at a temperature of about 30,000 K under conditions of coronal ionization equilibrium (Mazzotta et al. 1998), this range of temperatures is not sufficient for most diagnostic applications. Recently, Bray et al. (2000) have calculated He I collision strengths at temperatures between 5600 and 560,000 K using the convergent close-coupling method. When the two calculations are compared, there is often, but not always, a reasonable agreement in the temperature region where the two calculations overlap. For the $1s^2 - 1snp$ allowed transitions, the Bray calculations tend to the high temperature limit in a smooth manner. However, this does not appear to be the case for all allowed transitions. In combining the two sets of calculations, we have included all of the Sawey & Berrington (1993) collision strengths and the highest temperature value of the Bray et al. (2000) values. In our usual manner, the scaling laws of Burgess & Tully (1992) have been applied to the combined set of collision strengths and splines fit to the scaled collision strengths. Previously, Lanzafame et al. (1993) showed how the He I calculations could be extended to higher temperature by applying the same scaling laws for the allowed transitions.

5.3. Lithium isoelectronic sequence

5.3.1. C IV, O VI

The collisional data for the $n = 2, 3, 4$ configurations have been replaced with the R -matrix calculations from Griffin et al. (2000). These correspond to the 15 lowest energy levels in the atomic model for both ions.

The calculations were carried out using the R -matrix with pseudo-states method (RMPS Bartschat et al. 1996), including 9 spectroscopic terms of the configurations $1s^22s$, $1s^23s$, $1s^23p$, $1s^23d$, $1s^24s$, $1s^24p$, $1s^24d$ and $1s^24f$, and 32 pseudo states $1s^2nl$ for $n = 5$ to 12 and $l = 0$ to 3. Results showed that the presence of pseudo states affects mostly transitions to the $n = 4$ levels, and is less important for the transitions to lower levels.

Effective collision strengths are calculated in LS coupling, and they have been scaled into intermediate coupling by using the statistical weights of the levels. Effective collision strengths are provided by Griffin et al. (2000) in the $4.2 \leq \log T \leq 6.5$ temperature range for C IV, and in the $4.55 \leq \log T \leq 6.85$ temperature range for O VI (T in K).

The radiative and collisional data for additional transitions remain unchanged.

5.4. Beryllium isoelectronic sequence

In the earlier versions of the database, the collisional data for the $n = 2$ levels in the Be-like sequence were generally taken from the distorted wave calculations from Zhang & Sampson (1992). The only exceptions were Ne VII, Mg IX and the minor ions, for which Version 3 of the database adopted *R*-matrix results. However, it has been found that resonances play an important role in the calculation of Be-like $n = 2$ effective collision strengths (Landi et al. 2001), so the distorted wave data for the $n = 2$ transitions in the whole sequence have been replaced with close coupling results, as described below. The accuracy of the *R*-matrix data in the case of Ne VII was demonstrated from laboratory spectra by Mattioli et al. (1999).

5.4.1. O V, Si XI

C. Jordan (2001, private communication) noted that the O V $\lambda 1218/\lambda 1371$ line ratio calculated with the Version 2 distorted wave rates provided unusually high densities for the Sun, in disagreement with values from other ions formed at similar temperatures. The use of the Berrington et al. (1985) *R*-matrix results yielded more realistic density values, and so these data have been adopted in the present version of the database both for O V and Si XI.

The data consist of LS coupling effective collision strengths calculated for all transitions between the six $n = 2$ terms using the *R*-matrix method. Intermediate coupling effective collision strengths were obtained by scaling the Berrington et al. (1985) data with the statistical weights of the levels. Data are provided for the temperature range $4.5 \leq \log T \leq 6.1$ for O V and $5.4 \leq \log T \leq 7.0$ for Si XI. Although it is not easy to assess the quality of such calculations, Berrington et al. (1985) claim an accuracy of 10–20% for their results.

All other data for these two ions remain unchanged.

5.4.2. Al X

Collisional data for Al X have been taken from Keenan et al. (1986), who interpolated the *R*-matrix data of Berrington et al. (1985) for C III, O V, Ne VII and Si XI. Effective collision strengths are provided for transitions between all of the 10 fine structure $n = 2$ levels in the Al X model. Keenan et al. (1986) claim that their interpolated data are accurate to within 10 % over a temperature range of ± 0.08 dex from the maximum Al X fractional abundance in ionization equilibrium, corresponding to a temperature range of $5.3 \leq \log T \leq 6.9$ (T in K).

All other data for Al X remain unchanged.

5.4.3. *S XIII, Ar XV*

Collisional data for S XIII and Ar XV have been taken from Keenan (1988) who interpolated *R*-matrix data for Ne VII, Si XI (Berrington et al. 1985) and Ca XVII (Dufton et al. 1983). Effective collision strengths are provided for transitions between all of the 10 fine structure $n = 2$ levels. Keenan (1988) claims that these interpolated data are accurate to within 10% over a temperature range of ± 0.08 dex from the maximum fractional abundance of each ion, corresponding to $5.6 \leq \log T \leq 7.2$ for S XIII and $5.7 \leq \log T \leq 7.3$ for Ar XV. Keenan (1988) notes that for some transitions his results are significantly different from the distorted wave results of Bhatia et al. (1986).

All other data for these ions remain unchanged.

5.4.4. *Ca XVII*

Ca XVII collisional data for the $n = 2$ levels have been changed, in order to use the *R*-matrix results from Dufton et al. (1983). Effective collision strengths were calculated in LS coupling for all of the $n = 2$ levels, and then converted into intermediate coupling collisional data. At low impact energies, an extension of the *R*-matrix method was applied to take into account relativistic effects in the scattering equations. Effective collision strengths were provided in the $6.4 \leq \log T \leq 7.2$ temperature range. Oscillator strengths are also provided by Dufton et al. (1983), and these have been used to scale the effective collision strengths according to the Burgess & Tully (1992) scaling laws. Dufton et al. (1983) finds good agreement between his *R*-matrix results and the distorted wave calculations of Bhatia & Mason (1983).

All other data for Ca XVII remain unchanged.

5.4.5. *Fe XXIII*

Fe XXIII distorted wave collision rates for the $n = 2$ levels have been replaced by the *R*-matrix calculations carried out by Chidichimo et al. (1999) as part of the Iron Project. Effective collision strengths for the transitions were tabulated over the temperature range $6.3 \leq \log T \leq 8.1$.

Chidichimo et al. (1999) have compared their results with the distorted wave calculations from Zhang & Sampson (1992) and Bhatia & Mason (1986), finding that the background collision strengths were in good agreement in most cases. However, the neglect of resonances in the distorted wave data leads to large differences in some of the effective collision strengths.

5.5. Boron isoelectronic sequence

5.5.1. *Al IX, Si X, S XII, Ar XIV, Ca XVI*

Earlier versions of the CHIANTI database adopted the *R*-matrix calculations of Zhang et al. (1994) for transitions within the $n = 2$ levels. However, a small error has been found in the data (H.L. Zhang 2001, private communication), whose effect is small, but non-negligible for ions heavier than Al IX. Keenan et al. (2000) published revised collisional rates for Si X and compared them with the observations of a solar active region, demonstrating the accuracy of the new data.

In Version 4 of the database, we have adopted the revised values of the $n = 2$ electron excitation rates kindly made available to us by Dr. H.L. Zhang, for all of the most abundant ions in the sequence that are affected by the correction in the calculation: Al IX, Si X, S XII, Ar XIV and Ca XVI. The data were calculated using the *R*-matrix method for a large range of temperatures, from $T/z^2=100$ to 50000 (T in K), where $z = 8$ (Al IX), 9 (Si X), 11 (S XII), 13 (Ar XIV) and 15 (Ca XVI).

All other data are left unchanged.

5.5.2. *Fe XXII*

The *R*-matrix calculations from Zhang et al. (1994) have been superseded by an extensive computation carried out by Badnell et al. (2001). The atomic model includes a total of 20 configurations, giving rise to 204 fine structure levels. The configurations included are $2s^22p$, $2s2p^2$, $2p^3$, $2s^2nl$, $2s2pnl$ and $2p^2nl$ where $n = 3$ and $l = s, p, d$; and $n = 4$ and $l = s, p, d, f$.

Observed energy levels are taken from Shirai et al. (2000) and Kelly (1987). Theoretical energy levels, radiative decay rates and effective collision strengths for all the levels in the atomic model come from Badnell et al. (2001). The observed energies of a few levels have been interchanged to match the ordering of the theoretical energies. Einstein coefficients for a few forbidden transitions within the ground configuration, not available in Badnell et al. (2001), were taken from Galavís et al. (1998); a comparison between the Badnell et al. (2001) and Galavís et al. (1998) radiative rates for common transitions shows that the two calculations agree to within 10%.

Badnell et al. (2001) carried out *R*-matrix calculations of collision strengths using the Intermediate Coupling Frame Transformation method (ICFT; Griffin et al. 1998) for all possible transitions in the atomic model. Effective collision strengths are provided for temperatures in the range $4.99 \leq \log T \leq 6.99$. However, Badnell et al. (2001) warn that data for $n = 3$ and 4 levels at temperatures lower than 2.4×10^6 K are less reliable, and so these low temperature data have not been considered for inclusion in the database. The Badnell et al. (2001) dataset is the most extensive available in the literature; we also note that Zhang & Pradhan (1997) have carried out a relativistic *R*-matrix calculation for collisional excitation rates for the first 45 levels in the Fe XXII

model as part of the Iron Project.

5.6. Carbon isoelectronic sequence

5.6.1. *Ne V*

Radiative and collisional data for 49 fine structure levels of Ne V have been calculated by Griffin & Badnell (2000) using the ICFT method within the *R*-matrix approximation. 46 levels belong to the $2s^22p^2$, $2s2p^3$, $2p^4$, $2s^22p2l$ ($l = s, p, d$), and the remaining levels belong to the $2s2p^23s$ 5P term. The effective collision strengths cover the temperature range $3.0 \leq \log T \leq 6.0$.

Griffin & Badnell (2000) did not provide the forbidden radiative decay rates for the ground configuration and so we have adopted the data provided by Bhatia & Doschek (1993), except for the $^3P_{1,2} - ^1D_2$ transitions which come from Storey & Zeippen (2000).

Experimental energy levels are available for all 49 fine structure levels in the model; $n = 2$ level energies are taken from Edlen (1985), while for all other levels the values from the NIST database (Fuhr et al. 1999) are used.

5.6.2. *Fe XXI*

The Fe XXI atomic model in Version 3.02, that included 68 fine structure levels arising from 9 different configurations, has been increased to 290 fine structure levels from 18 configurations. These are the $2s^22p^2$, $2s2p^3$, $2p^4$, $2s^22p3l$, $2s2p^23l$, $2p^33l$ ($l = s, p, d$), $2s^22p4l$ ($l = s, p, d, f$) and $2s^22p5l$ ($l = s, d$) configurations. Experimental energies are available only for a few levels and their values come from Shirai et al. (2000); additional energies are taken from Mason et al. (1979), Bromage et al. (1977), Kelly (1987) and the laboratory measurements of Brown et al. (2002).

The Fe XXI dataset comes from three different sources, each providing a complete set of theoretical energy levels, radiative coefficients and collision rates. Data for the levels belonging to the $2p^33l$ configurations are taken from Zhang & Sampson (1997), data for $n = 5$ configurations come from Phillips et al. (1996), while for all the other levels we have adopted the recent Badnell & Griffin (2001) dataset.

Badnell & Griffin (2001) provided radiative data for all possible transitions within the lowest 200 levels of the present Fe XXI model, with the only exceptions the forbidden transitions between levels in the ground configuration; for these, radiative data have been calculated using the program SSTRUCT (Eissner et al. 1974). The Badnell & Griffin (2001) collision rates have been calculated using the *R*-matrix method in conjunction with the ICFT method; effective collision strengths are provided in the temperature range $4.9 \leq \log T \leq 7.9$. However, due to the uncertainties in the calculation of the $n > 2$ level energies, effective collision strengths are recommended only for

temperatures greater than 2×10^6 K.

Both Zhang & Sampson (1997) and Phillips et al. (1996) calculate collision strengths under the distorted wave approximation; both authors also provide data for many more levels and transitions, for which results from Badnell & Griffin (2001) are also available. As noted by Badnell & Griffin (2001), resonances play a major role in the collisional excitation rates for these levels, and consequently *R*-matrix results are considered more accurate and have been preferred.

Recently, also Butler & Zeippen (2000) carried out extensive *R*-matrix calculations for Fe XXI as part of the Iron Project, including $n = 2$ and $n = 3$ levels. However, the larger target representation adopted by Badnell & Griffin (2001) allows the inclusion of important resonances that significantly affect several $n = 2 \rightarrow n = 2, 3$ transitions, and so the latter results have been preferred. On the contrary, comparison with results from Phillips et al. (1996) for the $n = 4$ levels shows good agreement, demonstrating that resonances are unimportant for transitions from these levels.

Fig. 2b demonstrates the difference between the Fe XXI $\lambda 102/\lambda 128$ density diagnostic ratio calculated with this new model of the ion (with and without proton rates), and with the previous version of CHIANTI.

5.7. Nitrogen isoelectronic sequence

5.7.1. NI

The CHIANTI atomic model for N I includes 26 fine structure levels arising from 4 different configurations: $2s^22p^3$, $2s2p^4$, $2s^22p^23s$ and $2s^22p^23p$. Experimental energies come from the NIST database (Fuhr et al. 1999) and are available for all 26 levels.

Theoretical energy levels and radiative data come from the calculations of Hibbert et al. (1991), carried out using the CIV3 code of Hibbert (1975). Hibbert et al. (1991) provide *A* values for transitions between the ground and excited configurations, and between two excited configurations, in intermediate coupling. Data for forbidden transitions within the ground configurations were taken from the NIST database. It is to be noted that Tayal & Beatty (1999) calculated oscillator strengths for all transitions among the $2s^22p^3$, $2s2p^4$, $2s^22p^23l$ ($l = s, p, d$) configurations, but provided only LS coupling results. However, Tayal & Beatty (1999) report good agreement between their results and earlier calculations, including Hibbert et al. (1991).

Tayal (2000) calculated fine-structure effective collision strengths for transitions within the ground configuration and from the ground to the excited configuration levels in the CHIANTI model. Tayal (2000) adopted the *R*-matrix approximation, including 18 LS states in the target representation. Data are provided in the temperature range $3.0 \leq \log T \leq 5.75$.

It is to be noted that the effective collision strengths of the $2s^22p^3$ $^4S_{3/2} - 2s^22p^23p$ $^2D_{3/2}$

and $^2D_{5/2}$ transitions tabulated in Tayal (2000) were incorrect; the author has kindly provided us revised values.

5.7.2. O II

All radiative data for the ground $2s^22p^3$ configuration of O II have been updated with the calculations of Zeippen (1987). We note that two errors in the earlier model of O II have been corrected: the A value for the $2s^22p^3\ ^4S_{3/2}-^2D_{3/2}$ transition had inadvertently been assigned to the $2s^22p^3\ ^4S_{3/2}-^2D_{5/2}$ transition, and vice versa. The same error also occurred for the $2s^22p^3\ ^4S_{3/2}-^2P_{1/2}$ and $^4S_{3/2}-^2P_{3/2}$ transitions. The $^4S-^2D$ transitions give rise to the prominent density diagnostic ratio $\lambda 3726/\lambda 3729$ for nebular plasmas (Seaton & Osterbrock 1957), and the corrections to the CHIANTI model now give excellent agreement to earlier work on this ratio (e.g., Stanghellini & Kaler 1989).

5.7.3. Mg VI, Al VII, P IX, K XIII, Ca XIV, Cr XVIII, Mn XIX, Co XXI, Ni XXII

The CHIANTI models for these ions have been updated with the data of Zhang & Sampson (1999) who provide collision strengths, theoretical energy levels and oscillator strengths for all transitions between the 15 levels of the $2s^22p^3$, $2s2p^4$ and $2p^5$ configurations, increasing the number of transitions predicted by the CHIANTI models. The collision strengths were calculated at six values of the incoming electron energy, and 5 point spline fits were performed to the 105 transitions of each ion to an accuracy of $\lesssim 1\%$.

A values for the forbidden transitions in the ions have been taken from Merkelis et al. (1999) where available, and Zhang & Sampson (1999) otherwise. Oscillator strengths and A values for allowed transitions are from Zhang & Sampson (1999). Experimental values of the 15 energy levels of each ion were obtained from Edlen (1984).

We have compared the radiative data with those present in the previous version of CHIANTI and the few values available in the NIST database (Fuhr et al. 1999), and have found only small differences (within 10–20%) for most transitions. In earlier versions of CHIANTI the data for Al VII, P IX, K XIII, Cr XVIII, Co XXI and Ni XXII had been derived through interpolation of the data-sets of neighbouring ions on the isoelectronic sequence (Landi et al. 1999). The good agreement of the data-sets confirms the validity of the interpolation procedure adopted in v.2 of CHIANTI.

For Mg VI, the additional data for the $2s^22p^23s$ configuration of Bhatia & Young (1998) described in Landi et al. (1999) have been retained.

5.7.4. Si VIII

The new CHIANTI model for Si VIII contains all 72 levels of the $2s^22p^3$, $2s2p^4$, $2p^5$ and $2s^22p^23l$ ($l = s, p, d$) configurations. For transitions amongst the levels of the ground $2s^22p^3$ configuration, the R -matrix data of Bell et al. (2001) are used. The authors tabulated Maxwellian-averaged collision strengths for temperatures $3.3 \leq \log T \leq 6.5$, and these data were fitted with nine point splines. In order to achieve an accuracy of $\lesssim 1\%$ in the fits it was necessary to omit the two lowest temperature data points, and so the fits apply to the temperature range $3.7 \leq \log T \leq 6.5$. The new R -matrix data modify the Si VIII ground configuration line emissivities by $\sim 10\%$ compared with the Zhang & Sampson (1999) distorted wave data. For all remaining $n = 2$ transitions, the distorted wave collision strengths of Zhang & Sampson (1999) were used.

Bhatia & Landi (2002a) have calculated collision strengths for transitions involving the $n = 3$ levels using the University College of London distorted wave programs (Eissner & Seaton 1972; Eissner 1998). The collision strengths were calculated at incident electron energies of 20, 40, 60 and 80 Ry.

Radiative data for forbidden transitions are from Merkleis et al. (1999) and all other $n = 2$ radiative data are from Zhang & Sampson (1999). For transitions involving the $n = 3$ levels, radiative data are from Bhatia & Landi (2002a). Experimental energies for the $n = 2$ levels are from Edlen (1984), while $n = 3$ energies have been compiled from the NIST database (Fuhr et al. 1999) and Kink et al. (1999). For a number of the $n = 3$ levels experimental energies were unavailable and for these the theoretical values of Bhatia & Landi (2002a) have been used.

The extension of the CHIANTI Si VIII model to include the $n = 3$ levels is particularly important as a number of $n = 3$ to $n = 3$ transitions have been identified in solar and laboratory spectra between 900 and 1300 Å (Kink et al. 1999). A number of ground forbidden transitions are also found in this wavelength range, and ratios between the two sets of lines have considerable diagnostic potential.

5.7.5. SX

Bell & Ramsbottom (2000) have published Maxwellian-averaged collision strengths for all 231 possible transitions amongst the 22 levels of the $2s^22p^3$, $2s2p^4$, $2p^5$ and $2s^22p^23s$ configurations, calculated in the R -matrix approximation. The values are tabulated for 12 temperatures over the range $4.6 \leq \log T \leq 6.7$ and have been fitted with 5 point or 9 point splines to yield fits accurate to $\lesssim 1\%$. For five transitions, errors were found in the original tabulated data and have been corrected. More details are provided in the comments section of the CHIANTI .SPLUPS file.

Radiative data are from Merkleis et al. (1999) for the forbidden transitions and Zhang & Sampson (1999) for all other $n = 2$ transitions. No data were available in the literature for the $n = 3$ levels and so SSTRUCT was used to derive oscillator strengths and decay rates. The model

used contained 24 configurations and showed excellent agreement with the data of Merkelis et al. (1999) and Zhang & Sampson (1999) for the $n = 2$ levels.

Experimental energies are available for all 22 levels and we use the values of Edlen (1984) for the $n = 2$ levels, and the values from the NIST database (Fuhr et al. 1999) for the $2s^22p^23s$ levels. The level ordering of Bell & Ramsbottom (2000) for the $n = 2$ configurations has been modified to be consistent with the other nitrogen-like ions, and follows the experimental level ordering of Edlen (1984). The new CHIANTI model for S X includes lines around 50 Å due to $2s^22p^3-2s^22p^23s$ transitions which were not present in earlier versions of the database. We have compared $n = 2$ line emissivities computed with the new model with the previous one (based on the calculations of Bhatia & Mason 1980b) and found differences of the order of 20–30%, the largest being for the transitions $2s^22p^3\ ^4S_{3/2}-2s2p^4\ ^4P_J$ which give rise to emission lines between 314 and 320 Å.

5.7.6. Ar XII, Ti XVI, Zn XXIV

The atomic data for the $n = 2$ levels of Ar XII, Ti XVI and Zn XXIV are from the same sources as described in Sect. 5.7.3: Zhang & Sampson (1999) for the collisional data, Merkelis et al. (1999) and Zhang & Sampson (1999) for the radiative data, and Edlen (1984) for the experimental energy levels.

Additional data for the levels in the $2s^22p^23l$ ($l = s, p, d$) configurations have been published by Bhatia et al. (1989a), extending the CHIANTI models to 72 fine structure levels. Bhatia et al. (1989a) calculated collision strengths at a single energy for all transitions from the five levels of the ground $2s^22p^3$ configuration. In addition they calculated oscillator strengths and A values for all allowed transitions from the $n = 3$ levels. Experimental energy levels are from the NIST database (Fuhr et al. 1999). For some levels, experimental energies were unavailable and the theoretical energies of Bhatia et al. (1989a) were used.

5.7.7. Fe XX

The previous atomic model for Fe XX included the $n = 2$ Bhatia & Mason (1980a) and $n = 3$ Bhatia et al. (1989a) calculations, for a total of 72 levels. This model has been improved by including the new R -matrix calculations of Butler & Zeippen (2001a), produced as part of the Iron Project. The authors present complete collisional and radiative data for 86 levels within the $n = 2$ and $n = 3$ configurations. Maxwellian-averaged collision strengths were tabulated for 27 temperatures between $\log T = 5.0$ and $\log T = 7.6$. All of the electron impact excitation data from the ground configuration have been fitted with 9 point splines, making sure that the fits were good to $\lesssim 1\%$ over the temperature range of the original calculation.

Experimental energy levels are from a variety of sources. For the $2s^22p^3$ ground configuration

the values of Kucera et al. (2000) are used, while for all other levels in the $n = 2$ configurations Edlen (1984) is used. A number of $n = 3$ level energies have been derived from the recent line list of Brown et al. (2002). Further $n = 3$ energies are from Shirai et al. (2000), Kelly (1987) and Phillips et al. (1999).

The extensive line list compiled Brown et al. (2002) from laboratory plasmas reports a number of Fe XX spectral lines that allow to determine the energies of many levels previously unavailable. A few additional level energies has been identified from Phillips et al. (1999). These new values have been used in the present version of the database to complement the energy values already included in the CHIANTI Version 3 model.

The inclusion of these energies in CHIANTI allows the assignment of laboratory-based wavelengths to many strong transitions predicted by CHIANTI, so that these can be used for analysis.

Emissivities computed with the new Fe XX model show small differences (within 20%) compared to the previous CHIANTI model for transitions from the $2s2p^4$ and $2s^22p^23d$ configurations. For transitions from the $2s^22p^23s$ configuration, however, much larger differences of up to a factor 2 are found.

5.8. Oxygen isoelectronic sequence

5.8.1. Ne III

Bhatia et al. (2002a) have carried out *ab initio* calculations of energy levels, radiative data and collisional excitation rates for all levels in the $n = 2$ and $2s^22p^23l$ ($l = s, d$) configurations, for a total of 57 fine structure levels. Collision strengths were calculated at incident electron energies of 5, 15, 25, 35 and 45 Ry. These calculations were performed in the distorted wave approximation, so that the collision rates do not include resonances. For this reason, close-coupling effective collision strengths from McLaughlin & Bell (2000) have been used for the 10 transitions within the ground configuration. The authors calculated Maxwellian-averaged collision strengths from $\log T = 3.0$ to 6.0 at 0.2 dex intervals, and for several of the transitions it was necessary to use 9 point splines to fit the data in order to provide coverage over the full temperature range. Ne III gives rise to several strong forbidden lines in spectra of photoionized plasmas for which the electron temperature is well below that in collisional ionization equilibrium, and so it is important to provide accurate fits over a wide temperature range.

Experimental energies are available for most of the $n = 3$ levels, and come from the NIST database (Fuhr et al. 1999).

5.8.2. *S IX*

Several $n = 3 \rightarrow n = 3$ transitions have been identified in solar and laboratory spectra in the ultraviolet range between 700 Å and 1000 Å by Kink et al. (1997), Jupen & Engström (1997) and Feldman et al. (1997). These lines have a great diagnostic potential if used in conjunction with the forbidden lines in the ground $2s^22p^4$ configuration found in the same wavelength range. Their detection has triggered the calculation of atomic data and transition rates carried out by Bhatia & Landi (2002b). This calculation replaces the older distorted wave calculation of Bhatia et al. (1979) for the $n = 2$ levels used in earlier versions of CHIANTI.

Bhatia & Landi (2002b) include six different configurations in the S IX atomic model: $2s^22p^4$, $2s2p^5$, $2p^6$ and $2s^22p^33l$ ($l = s, p, d$), corresponding to 86 fine structure levels. Experimental energies are available for most of the levels, and have been taken from the NIST database (Fuhr et al. 1999), Kelly (1987) and Jupen & Engström (1997); the experimental energies of two levels have been exchanged in order to correctly match the theoretical levels.

Theoretical energy levels, radiative data and collision strengths are provided by Bhatia & Landi (2002b) for all levels and transitions in the atomic model. Collision strengths have been calculated for five values of the incident electron energy: 25, 50, 75, 100 and 125 Ry. Comparison between these collision strengths and the earlier values from Bhatia et al. (1979) show a reasonable agreement, although some differences are found due to the more accurate target representation adopted by Bhatia & Landi (2002b).

5.8.3. *Fe XIX*

Butler & Zeippen (2001b) have carried out a complete calculation of energy levels, radiative data and collisional rates for Fe XIX, as part of the Iron Project. This is the first calculation for Fe XIX to adopt the *R*-matrix approximation, thus enabling important resonant contributions to be accounted for. All earlier calculations were performed under the distorted wave approximation.

Butler & Zeippen (2001b) provide data for the $2s^22p^4$, $2s2p^5$, $2p^6$, $2s^22p^33l$ ($l = s, p, d$) configuration, as well as for the two lowest-lying triplets of the $2s2p^43s$ configuration. The atomic model thus includes 92 fine structure levels.

Experimental energies are taken from Shirai et al. (2000) and Kelly (1987), but are available only for the $n = 2$ and a few of the $n = 3$ levels. Recent laboratory measurements of Fe XIX X-ray lines (Brown et al. 2002) allow the determination of several new level energies, and these have been added to the CHIANTI model. An additional energy value has also come from Phillips et al. (1999). Theoretical energies, as well as radiative data, are provided by Butler & Zeippen (2001b) for all levels and transitions except for the transitions within the ground configuration, for which data are taken from Loulorgue et al. (1985).

Maxwellian-averaged collision strengths were provided by Butler & Zeippen (2001b) over the temperature range $5.0 \leq \log T \leq 7.6$. The authors claim accuracy of the $n = 2$ collision rates to better than 20%, but for transitions involving the $n = 3$ levels resonances coming from $n = 4$ levels and beyond are omitted and so the rates are less accurate. Comparison between collision strengths from Butler & Zeippen (2001b) and the distorted wave calculations by Zhang & Sampson (2001) and Bhatia et al. (1989b) show good agreement in the energy regions where no resonances are present.

5.8.4. *Ni XXI*

Although Ni XXI gives rise to several strong allowed transitions, there have been no calculations of electron excitation rates in the literature and so it has not been possible to include the ion in the previous versions of CHIANTI. Recently, however, Bhatia et al. (2002b) calculated a complete set of energy levels, radiative decay rates and collision strengths for 58 fine structure levels from the $2s^22p^4$, $2s2p^5$, $2p^6$, $2s^22p^33l$ ($l = s, d$) configurations and this data-set is now included in CHIANTI. Collision strengths have been calculated in the distorted wave approximation at incident electron energies of 85, 170, 255, 340 and 425 Ry. Experimental energy levels are available for all the $n = 2$ levels and a few $n = 3$ levels, and they are taken from Shirai et al. (2000).

5.9. Fluorine isoelectronic sequence

5.9.1. *Fe XVIII*

The previous Fe XVIII CHIANTI model (Dere et al. 1997) contained distorted wave calculations from Sampson et al. (1991) for all transitions. The ground $2s^22p^5$ $^2P_{1/2} - ^2P_{3/2}$ transition data have now been replaced with the close-coupling calculations of Berrington et al. (1998) who tabulate Maxwellian-averaged collision strengths for 11 temperatures over the range $5.5 \leq \log T \leq 7.5$. The new data serve to increase the emissivity of the Fe XVIII ground transition at $\lambda 974.86$ by around 50% (Fig. 2). This line has recently been observed in stellar spectra (Young et al. 2001).

5.10. Magnesium isoelectronic sequence

5.10.1. *Fe XV*

In the recent past, there has been a considerable effort to calculate accurate collision rates for Fe XV. Independent calculations have been made available by a number of authors, using the *R*-matrix approach in all cases but one. Eissner et al. (1999), Griffin et al. (1999a) and Aggarwal et al. (1999) use different variations of the same *R*-matrix approach, while Bhatia et al. (1997)

adopted the distorted wave approximation. Aggarwal et al. (2000) report a comparison between the three *R*-matrix calculations listed above for the lowest 10 levels, and find that the values of the collisional data for Aggarwal et al. (1999) and Eissner et al. (1999) are in very good agreement, while those from Griffin et al. (1999a) show some unexpected problems. Corrections to the Griffin et al. (1999a) collisional data have been provided by the same authors in a later note (Griffin et al. 1999b).

In CHIANTI, we have adopted a combination of data from Eissner et al. (1999), Griffin et al. (1999a,b) and Bhatia et al. (1997). The atomic model includes 53 fine structure energy levels, coming from 11 configurations. Experimental energy levels come mainly from Shirai et al. (2000), although additional energies are taken from Eissner et al. (1999) and Reader & Sugar (1975).

Data for the $n = 3$ configurations are taken from Eissner et al. (1999): these include the 35 lowest energy levels. Theoretical energies and effective collision strengths are provided by the authors; however, no radiative data is available. *A* values and oscillator strengths have been calculated using SSTRUCT by one of the authors (E. Landi) for all 53 levels in the CHIANTI model using a 21-configuration model. Comparison of the SSTRUCT results with the Griffin et al. (1999a) *A* values for $n = 4$ levels yields good agreement. Eissner et al. (1999) provide Breit-Pauli *R*-matrix effective collision strengths for temperatures in the range $5.0 \leq \log T \leq 7.0$.

Theoretical energies, radiative data and effective collision strengths for the $3s4l$ ($l = s, p, d$) levels and transitions are taken from the corrected calculations of Griffin et al. (1999b). Effective collision strengths are calculated using the ICFT *R*-matrix method, and are provided in the temperature range $5.05 \leq \log T \leq 7.05$.

Data for the high energy $3p4s$ and $3s4f$ configurations are taken from the distorted wave calculations of Bhatia et al. (1997). Radiative data were computed using SSTRUCT, while collision strengths were calculated using the University College of London DW code for three incident electron energies: 25, 50 and 75 Ry. It is to be noted that Bhatia et al. (1997) neglected the $3d^2$ configuration and this constitutes the main deficiency of their data for these two configurations.

5.11. Phosphorus isoelectronic sequence

5.11.1. SII

The collisional data of Cai & Pradhan (1993) have been replaced with the more recent results of Ramsbottom et al. (1996). These authors calculated Maxwellian-averaged collision strengths for transitions between forty-three levels of the $3s^23p^3$, $3s3p^4$, $3s^23p^23d$, $3s^23p^24s$ and $3s^23p^24p$ configurations of S II. Ramsbottom et al. (1996) tabulate their collision strengths for temperatures $3.5 \leq \log T \leq 5.0$, however data was provided to CHIANTI by the authors over the extended range $3.0 \leq \log T \leq 6.4$. When fitting the data over this range with the Burgess & Tully (1992) method it was found for a number of the allowed transitions that the collision strengths did not

tend towards the high temperature limit point. This is due to the geometric series approximation to the partial collision strengths failing at high electron energies (C.A. Ramsbottom 2001, private communication). For this reason the temperature range $3.0 \leq \log T \leq 5.5$ was considered for the fitting. Only transitions involving the five levels of the ground $3s^23p^3$ configuration, and the metastable $3s^23p^33d\ ^4F_{9/2}$ were fitted. 9 point splines were used for those data that were difficult to fit with 5 point splines, however it was still found necessary to omit data points from the fit in some cases in order to obtain fits accurate to $\lesssim 1\%$. In summary the fits in CHIANTI accurately represent all of the original data over the temperature range $3.3 \leq \log T \leq 5.1$. For many of the transitions, however, the fits are accurate over a wider temperature range.

A complete set of radiative data for the 43 levels of the Ramsbottom et al. (1996) calculations have never been published. S. Nahar (2001, private communication) has, however, computed radiative decay rates for all of the allowed transitions between these levels and they have been included in the CHIANTI model. The calculations are an extension of those presented in Nahar (1998). For the forbidden transitions amongst levels in the ground configuration and from the $3s^23p^33d\ ^4F_{9/2}$ level, the decay rates from earlier versions of CHIANTI have been retained (Dere et al. 1997). Additional forbidden decay rates have been computed by P.R. Young using a 24 configuration model input to the code SSTRUCT.

Experimental energy values for all of the 43 levels in the CHIANTI model have been obtained from the NIST database Fuhr et al. (1999).

Very significant differences are found between the present S II model and the one found in previous versions of CHIANTI. This is due to the inaccuracies in the Cai & Pradhan (1993) collisional data that have been highlighted by Ramsbottom et al. (1996) and Tayal (1997). The new CHIANTI model is found to provide excellent agreement with a far ultraviolet spectrum of the Jupiter-Io torus, which hosts a large number of $3s^23p^3-3s^23p^23d$ and $3s^23p^3-3s^23p^24s$ transitions (Feldman et al. 2001).

5.11.2. ArIV

Ar IV is a new addition to CHIANTI, and the model includes 30 fine structure levels from the $3s^23p^3$, $3s3p^4$ and $3s^23p^23d$ configurations. Experimental energies are taken from the NIST database (Fuhr et al. 1999) and are available for all but two of the Ar IV levels.

Ar IV radiative data have been calculated by one of the authors (E. Landi) with the SSTRUCT code, using a 24-configuration atomic model. A values have been corrected for the differences between computed and experimental energy levels; where no values were available, original results have been retained. A values and oscillator strengths have been compared with a number of earlier calculations, carried out with more limited atomic models and different codes. Forbidden transitions within the ground configuration have been compared with the computation of Mendoza & Zeippen (1982), Fritzsche et al. (1999) and Huang (1984) and good agreement was found. Optically allowed

oscillator strengths have been compared with the values from Fawcett (1986): the agreement is fairly good for most transitions, although in some cases significant differences arise.

Collisional data are taken from the *R*-matrix computations of Ramsbottom et al. (1997) for transitions within the ground configuration, and Ramsbottom & Bell (1997) for all other transitions. Calculations were carried out including a 13 LS state target model, and effective collision strengths were provided in the temperature range $3.0 \leq \log T \leq 6.0$. Comparison with the earlier close-coupling calculations for forbidden transitions in the ground configuration from Zeippen et al. (1987) outlines significant differences for many transitions, especially at low temperatures where resonance effects are greatest. These differences are probably due to the smaller number of terms included in the Zeippen et al. (1987) target representation. Comparison of Ar IV lines with observations in optical spectra from planetary nebulae confirms the accuracy of the adopted collisional data (Keenan et al. 1997).

5.11.3. *Fe XII*

Recently, Binello et al. (2001) have reported a new set of atomic structure calculations for Fe XII. The resulting theoretical energy levels and radiative data represent an improvement relative to the earlier data of Binello et al. (1998a,b), and they are adopted in the present version of CHIANTI.

5.12. Scandium isoelectronic sequence

5.12.1. *Fe VI*

The CHIANTI atomic model for Fe VI includes 80 fine-structure levels, coming from the $3d^3$, $3d^24s$ and $3d^24p$ configurations. Experimental energy levels, taken from the NIST database (Fuhr et al. 1999) are available for all the levels in the adopted model.

Radiative data and theoretical energies are taken from the SSTRUCT calculation carried out by Chen & Pradhan (2000) as part of the Iron Project. Theoretical energies and A values are available for all levels and transitions in the atomic model. Comparison of both energies and A values with results from Bautista (1996) and Nussbaumer & Storey (1978) shows good agreement.

Effective collision strengths for all possible transitions in the adopted model have been calculated by Chen & Pradhan (1999). The *R*-matrix method has been used, and effective collision strengths have been calculated for the temperature range $4.0 \leq \log T \leq 6.0$. The authors also investigate the importance of relativistic effects and the effects of numerical uncertainties associated with the resolution of extensive resonances, finding that they are small.

6. Continuum

An IDL routine to include the two photon continuum has been added to CHIANTI, while the free-free (bremsstrahlung) and free-bound (radiative recombination) continua routines have been revised. Fig. 6 shows the total continuum spectrum at a temperature of 1×10^7 K computed for solar photospheric abundances with the Mazzotta et al. (1998) ionization balance. For comparison, the continuum given by the CONFLX.PRO procedure found in the Solarsoft⁷ package is also shown. This routine makes use of the analytic approximations for the continua presented in Sect. 4 of Mewe et al. (1986), and is commonly used for the interpretation of solar continuum measurements. Agreement is generally excellent with the differences lying largely in the improved treatment of the free-bound continuum.

6.1. Two photon continuum

6.1.1. Transitions in hydrogen-sequence ions

The first excited level ($2s\ ^2S_{1/2}$) of the hydrogen iso-electronic sequence ions can decay only by means of forbidden magnetic dipole and two-photon transitions. The importance of the competing magnetic dipole transition increases with Z but for nickel ($Z = 28$), the two-photon transition rate is roughly 5 times that of the magnetic dipole rate.

The spectral emissivity (erg cm⁻³ s⁻¹ sr⁻¹ Å⁻¹) for optically-thin two-photon emission at wavelength λ is given by:

$$\frac{d\epsilon_{i,j}}{d\lambda} = \frac{hc}{4\pi\lambda} A_{ji} N_j(X^{+m}) \phi(\lambda_0/\lambda) \quad (11)$$

where $A_{j,i}$ (sec⁻¹) is the Einstein spontaneous emission coefficient (A value); $N_j(X^{+m})$ is the number density of the level j of the ion X^{+m} ; ϕ is the spectral distribution function; and λ_0 is the wavelength corresponding to the energy difference between the excited and ground level.

The transition rates for both the magnetic dipole and two-photon transitions are taken from Parpia & Johnson (1982). Tables of the spectral distribution function have been provided by Goldman & Drake (1982) for $Z = 1, 20, 40, 60, 80$ and 92 . Interpolation for values of $Z \leq 28$ should be fairly accurate.

⁷Solarsoft is a set of integrated software libraries, data bases, and system utilities that provide a common programming and data analysis environment for Solar Physics. It is available at <http://www.lmsal.com/solarsoft/>.

6.1.2. Two-photon continuum transitions in helium-sequence ions

For the helium iso-electronic sequence, the second excited level ($1s2s\ ^1S_0$) decays through a forbidden magnetic dipole and two-photon transitions. The two-photon decay rate has been calculated by Drake (1986). The two-photon spectral distribution has been calculated by Drake, Victor & Dalgarno (1969) for values of Z between 2 and 10. For values of Z higher than 10, we have used the spectral distribution for $Z = 10$. The shape of the distribution function does not appear to be changing rapidly with Z at $Z = 10$ so this extrapolation should be moderately accurate.

6.2. Bremsstrahlung

Itoh et al. (2000) have provided an analytical fitting formula for the relativistic thermal bremsstrahlung gaunt factors, and this is now added to CHIANTI. The fitting formula is valid for the ranges $6.0 \leq \log T \leq 8.5$ and $-4.0 \leq \log(hc/k\lambda T) \leq 1.0$. For temperatures below $\log T = 6.0$ we retain the non-relativistic Gaunt factors of Sutherland (1998) for computing the continuum. The condition $\log(hc/k\lambda T) \leq 1.0$ results in some of the low wavelength points being inaccurately represented by the Itoh et al. fitting formula. For these wavelengths the Gaunt factors of Sutherland (1998) are used to compute the continuum level.

The relativistic free-free continuum is almost identical to the non-relativistic continuum at low temperatures. At $T = 1 \times 10^8$ K (the maximum temperature permitted by the ion balance calculations contained in CHIANTI) the relativistic continuum is around 1% higher near the peak of the distribution.

The IDL procedure for calculating the bremsstrahlung emission (FREEFREE.PRO) retains the same name and is called in an identical way to the previous version.

6.3. Free-bound continuum

The method of calculating the free-bound continuum in version 3 of CHIANTI was due to Rybicki & Lightman (1979), setting the bound-free gaunt factors to unity. We have revised this significantly by now including accurate ground photoionization cross-sections and, for excited levels, using the gaunt factors of Karzas & Latter (1961).

The free-bound continuum emissivity produced from recombination onto an ion of charge Z can be written as

$$P_{fb,\lambda} = 3.0992 \times 10^{-52} N_e N_{Z+1} \frac{E_\lambda^5}{T^{3/2}} \sum_i \frac{\omega_i}{\omega_0} \sigma_i^{bf} \exp\left(-\frac{E_\lambda - I_i}{kT}\right) \quad [\text{erg cm}^{-3} \text{ s}^{-1} \text{ \AA}^{-1}] \quad (12)$$

where N_e and N_{Z+1} are the number densities of electrons and recombining ions, respectively, in

units of cm^{-3} ; E_λ is the energy in cm^{-1} of the emitted radiation; T is the plasma temperature in K; ω_i is the statistical weight of the level i in the recombined ion; ω_0 is the statistical weight of the ground level of the recombining ion; σ_i^{bf} is the photoionization cross-section from the level i in the recombined ion to the ground level of the recombining ion, in units of Mb ($= 10^{-18} \text{ cm}^2$); I_i is the ionization energy in units of cm^{-1} from the level i in the recombined ion; and k is the Boltzmann constant. The photoionization cross-section, σ_i^{bf} , is zero for photon energies $E_\lambda < I_i$. The sum in Eq. 12 is over all levels i below the recombined ion’s ionization limit. Within CHIANTI we take levels to be individual configurations within an ion rather than the usual fine structure levels employed in CHIANTI. Accurate photoionization cross-sections for transitions from the ground level are readily available in the literature, and we use the analytic fits of Verner & Yakovlev (1995) that are available for all ions of all elements up to zinc.

Cross-sections for photoionizations from excited levels are generally not available, and for these we use the hydrogenic approximation of Karzas & Latter (1961) where

$$\sigma_i^{\text{bf}} = 1.075812 \times 10^{-1} \frac{I_i^2 g_{\text{bf}}}{n_i E^3} \quad [\text{Mb}] \quad (13)$$

where I_i is the ionization energy of level i , g_{bf} is the bound-free gaunt factor, and n_i is the principal quantum number of the ejected electron. Tables of the gaunt factors as a function of energy for nl -resolved levels up to $n = 6$ and $l = 5$ are published in Karzas & Latter (1961).

As the ion levels considered for the free-bound continuum are different from those used in the level balance models for the ions, a new CHIANTI file, given the suffix .FBLVL, is introduced. This contains the configurations used for deriving the total free-bound emissivity for the ion. E.g., for C III with ground configuration $1s^2 2s^2 2p$, we included all configurations $1s^2 2s^2 nl$, with $nl = 2p, 3s, \dots, 5g$. For each configuration an energy is listed which is the weighted-average energy of all the fine structure levels in the configuration. For the low-lying configurations, these energies are derived from the data in the CHIANTI .ELVLC files. For higher-lying configurations the energies are derived in many cases from data in the NIST database. However for some ions, particularly the iron ions, complete energy level data is not available for $n = 4, 5, 6$ configurations and so theoretical data were used. Sources included atomic physics calculations already used in CHIANTI, TOPbase⁸, and theoretical models constructed with the SSTRUCT atomic code.

Only the most abundant elements are considered for the calculation of the free-bound continuum, and these are H, He, C, N, O, Ne, Mg, Al, Si, S, Ar, Ca, Fe and Ni. The contributions from all ions in CHIANTI of these elements are considered. Further ions not currently in CHIANTI have also been added, including Fe IV, Fe V and the neutrals C I, O I and Si I.

⁸A database containing results from The Opacity Project (Seaton 1987), available at <http://cdsweb.u-strasbg.fr/topbase.html>.

7. Summary

The previous sections have described the latest updates to the CHIANTI atomic database that will continue to make CHIANTI a vital tool for interpreting astrophysical data. The database and the associated IDL software package are freely available at three websites in the US and Europe:

- <http://wwwsolar.nrl.navy.mil/chianti.html>
- <http://www.arcetri.astro.it/science/chianti/chianti.html>
- <http://www.damtp.cam.ac.uk/user/astro/chianti/chianti.html>.

In addition, both the database and software package are available through the Solarsoft system (<http://www.lmsal.com/solarsoft/>).

We are grateful to our colleagues who have provided their data to us. These include A. K. Bhatia, S. Nahar, S. Tayal, and H. L. Zhang. We thank R.K. Smith for providing many proton rate data-sets in electronic format. We also acknowledge helpful discussions with C. Jordan and M. Copetti. The work of K. P. Dere and E. Landi was supported by NASA's Applied Information Systems Research Program and by a grant from the Chandra Emission Line Project. G. Del Zanna and H. E. Mason acknowledge support from PPARC. The CHIANTI team has benefited from a travel grant from NATO.

REFERENCES

- Aggarwal, K. M., Berrington, K. A., Burke, P. G., Kingston, A. E., & Pathak, A. 1991, J. Phys. B, 24, 1385
- Aggarwal, K. M., Deb, N. C., Keenan, F. P., & Msezane, A. Z. 1999, J. Phys. B, 32, 5257
- Aggarwal, K. M., Deb, N. C., Keenan, F. P., & Msezane, A. Z. 2000, J. Phys. B, 33, L391
- Akmal, A., Raymond, J. C., Vourlidas, A., Thompson, B., Ciaravella, A., Ko, Y.-K., Uzzo, M., & Wu, R. 2001, ApJ, 553, 922
- Alder, K., Bohr, A., Huus, T., Mottleson, B., & Winther, A. 1956, Rev. Mod. Phys., 28, 432
- Anderson, H., Ballance, C. P., Badnell, N. R., & Summers, H. P., 2000, J. Phys. B, 33, 1255
- Anderson, H., Ballance, C. P., Badnell, N. R., & Summers, H. P., 2002, J. Phys. B, submitted
- Badnell, N. R., & Griffin, D. C. 2001, J. Phys. B, 34, 681
- Badnell, N. R., Griffin, D. C., & Mitnik, D. M. 2001, J. Phys. B, 34, 5071

- Bahcall, J. N., & Wolff, R. A. 1968, *ApJ*, 152, 701
- Bartschat, K., Hudson, E. T., Scott, M. P., Burke, P. G. & Burke, V. M. 1996, *J. Phys. B*, 29, 115
- Bautista, M. A. 1996, *A&AS*, 119, 105
- Bautista, M. A., & Kallman, T. R. 2001, *ApJS*, 134, 139
- Beiersdorfer, P., Lepson, J. K., Brown, G. V., Utter, S. B., Kahn, S. M., Liedahl, D. A., & Mauche, C. W. 1999, *ApJ*, 519, L185
- Bell, K. L., & Ramsbottom, C. A. 2000, *At. Data Nucl. Data Tables*, 76, 176
- Bell, K. L., Matthews, A., & Ramsbottom, C. A. 2001, *MNRAS*, 322, 779
- Bely, O., & Faucher, P. 1970, *A&A*, 6, 88
- Berrington, K. A., Burke, P. G., Dufton, P. L., & Kingston, A. E. 1985, *At. Data Nucl. Data Tables*, 33, 195
- Berrington, K. A., Saraph, H. E., & Tully, J. A. 1998, *A&AS*, 129, 161
- Bhatia, A. K. 1982, *J. Appl. Phys*, 53, 59
- Bhatia, A. K., & Doschek, G. A. 1993, *At. Data Nucl. Data Tables*, 55, 315
- Bhatia, A. K., & Doschek, G. A. 1995, *At. Data Nucl. Data Tables*, 60, 97
- Bhatia, A. K. & Doschek, G. A. 1996, *At. Data Nucl. Data Tables*, 64, 183
- Bhatia, A. K., & Landi, E. 2002a, *At. Data Nucl. Data Tables*, in press
- Bhatia, A. K., & Landi, E. 2002b, *At. Data Nucl. Data Tables*, in press
- Bhatia, A. K., & Mason, H. E. 1980a, *A&A*, 83, 380
- Bhatia, A. K., & Mason, H. E. 1980b, *MNRAS*, 190, 925
- Bhatia, A. K., & Mason, H. E. 1983, *A&A*, 52, 115
- Bhatia, A. K., & Mason, H. E. 1986, *A&A*, 155, 413
- Bhatia, A. K., & Young, P. R. 1998, *At. Data Nucl. Data Tables*, 68, 219
- Bhatia, A. K., Feldman, U., & Doschek, G. A. 1979, *A&A*, 80, 22
- Bhatia, A. K., Feldman, U., & Doschek, G. A. 1980, *J. Appl. Phys.*, 51, 1464
- Bhatia, A. K., Feldman, U., & Seely, J. F. 1986, *At. Data Nucl. Data Tables*, 35, 449

- Bhatia, A. K., Seely, J. F., & Feldman, U. 1989a, At. Data Nucl. Data Tables, 43, 99
- Bhatia, A. K., Fawcett, B. C., Phillips, K. J. H., Lemen, J. R., Mason, H. E., 1989b, MNRAS, 240, 421
- Bhatia, A. K., Mason, H. E., & Blancard, C. 1997, At. Data Nucl. Data Tables, 66, 83
- Bhatia, A. K., Thomas, R. J., & Landi, E. 2002a, At. Data Nucl. Data Tables, in press
- Bhatia, A. K., Landi, E., & Mason, H. E. 2002b, At. Data Nucl. Data Tables, in press
- Binello, A. M., Mason, H. E., & Storey, P. J. 1998a, A&AS, 127, 545
- Binello, A. M., Mason, H. E., & Storey, P. J. 1998b, A&AS, 131, 153
- Binello, A. M., Landi, E., Mason, H. E., Storey, P. J., & Brosius, J. W. 2001, A&A, 370, 1071
- Brandt, J. C., et al. 2001, AJ, 121, 2999
- Bray, I., Burgess, A., Fursa, D. V., & Tully, J. A. 2000, A&AS, 146, 481
- Bromage, G. E., Cowan, R. D., Fawcett, B. C., Gordon, H., Hobby, M. G., Peacock, N. J., & Ridgeley, A. 1977, Culham Lab. Tech. Rep., 170
- Brosius, J. W., Davila, J. M., & Thomas, R. J. 1998, ApJ, 497, L113
- Brown, G. V., Beiersdorfer, P., Liedahl, D. A., Widmann, K., & Kahn, S. M. 1998, ‘ ApJ, 502, 1015
- Brown, G. V., Beiersdorfer, P., Liedahl, D. A., Widmann, K., Kahn, S. M., & Clothiaux, E. J 2002, ApJ, 140, 589
- Burgess A., & Tully J. A. 1992, A&A, 254, 436
- Butler, K., & Zeippen, C. J. 2000, A&AS, 143, 483
- Butler, K., & Zeippen, C. J. 2001a, A&A, 372, 1078
- Butler, K., & Zeippen, C. J. 2001b, A&A, 372, 1083
- Cai W., & Pradhan A. K., 1993, ApJS 88, 329
- Chen, G. X., & Pradhan, A. K. 1999, A&AS, 136, 395
- Chen, G. X., & Pradhan, A. K. 2000, A&AS, 147, 111
- Chidichimo, M. C., Zeman, V., Tully, J. A., & Berrington, K. A. 1999, A&AS, 137, 175
- Copeland, F., Reid, R. H. G., & Keenan, F. P. 1997, At. Data Nucl. Data Tables, 67, 179

- Dalgarno, A. 1983, in Atoms in Astrophysics, ed. P.G. Burke et al. (New York: Plenum), 103
- Del Zanna, G., Bromage, B. J. I., Landi, E., & Landini, M. 2001, A&A, 379, 708
- Del Zanna, G., Landini, M., & Mason, H. E. 2002, A&A, submitted
- Dere K. P., Landi E., Mason H. E., Monsignori Fossi B. C., & Young P. R., 1997, A&AS, 125, 149
- Dere, K. P., et al. 2000, Solar Phys., 195, 13
- Dere K. P., Landi E., Young P. R., & Del Zanna G. 2001, ApJS, 134, 331
- Dixon, W. V. D., Sallmen, S., Hurwitz, M., & Lieu, R. 2001, ApJ, 552, L69
- Doschek, G. A., Dere, K. P., Sandlin, G. D., Vanhoosier, M. E., Brueckner, G. E., Purcell, J. D., Tousey, R., & Feldman, U. 1975, ApJ, 196, L83
- Drake, G. W. F. 1986, Phys. Rev. A, 34, 2871
- Drake, G. W. F., Victor, G. A., & Dalgarno, A. 1969, Phys. Rev., 180, 25
- Dufton, P. L., Kingston, A. E., & Scott, N. S. 1983, J. Phys. B, 16, 3053
- Dupree, A. K., Brickhouse, N. S., Doschek, G. A., Green, J. C., & Raymond, J. C. 1993, ApJ, 418, L41
- Edlen, B. 1984, Phys. Scr., 30, 135
- Edlen, B. 1985, Phys. Scr., 31, 345
- Eissner, W., & Seaton, M. J. 1972, J. Phys. B, 5, 2187
- Eissner, W., Jones, M., & Nussbaumer, H. 1974, Comput. Phys. Commun., 8, 270
- Eissner, W. 1998, Comput. Phys. Commun., 114, 295
- Eissner, W., Galavís, M. E., Mendoza, C., & Zeippen, C. J. 1999, A&AS, 137, 165
- Faucher, P. 1975, J. Phys. B, 8, 1886
- Faucher, P. 1977, A&A, 54, 589
- Faucher, P. & Landman, D. A. 1977, A&A, 54, 159
- Faucher, P., Masnou-Seeuws, F. & Prudhomme, M. 1980, A&A, 81, 137
- Fawcett, B. C. 1986, At. Data Nucl. Data Tables, 35, 203
- Feldman, U., Doschek, G. A., Cheng, C. C., & Bhatia, A. K., 1980, J. Appl. Phys., 51, 190

- Feldman, U., Behring, W. E., Curdt, W., Schühle, U., Wilhelm, K., Lemaire, P., & Moran, T. M. 1997, *ApJS*, 113, 195
- Feldman, P. D., Ake, T. B., Berman, A. F., Moos, H. W., Sahnow, D. J., Strobel, D. F., Weaver, H. A., & Young, P. R. 2001, *ApJ*, 554, L123
- Flower, D. R. 1977, *A&A*, 54, 163
- Foster, V. J., Keenan, F. P., & Reid, R. H. G. 1994a, *At. Data Nucl. Data Tables*, 58, 227
- Foster, V. J., Keenan, F. P., & Reid, R. H. G. 1994b, *Phys. Rev. A*, 49, 3092
- Foster, V. J., Keenan, F. P., & Reid, R. H. G. 1997, *At. Data Nucl. Data Tables*, 67, 99
- Fournier, K. B., May, M. J., Liedahl, D. A., Pacella, D., Finkenthal, M., Leigheb, M., Mattioli, M., & Goldstein, W. H. 2001, *ApJ*, 561, 1144
- Fritzsche, S., Fricke, B., Geschke, D., Heitmann, A., & Sienkiewicz, J.E. 1999, *ApJ*, 518, 994
- Fuhr, J. R., et al. 1999, “NIST Atomic Spectra Database” ver. 2.0 March 1999. NIST Physical Reference Data. http://physics.nist.gov/cgi-bin/AtData/main_asd
- Galavís, M.E., Mendoza, C., & Zeippen, C.J. 1998, *A&AS*, 131, 499
- Goldman, S. P., & Drake, G. W. F. 1981, *Phys. Rev. A*, 24, 183
- Grevesse, A. & Sauval, A. J. 1998, *Space Sci. Rev.*, 85, 161
- Griffin, D. C., & Badnell, N. R. 2000, *J. Phys. B*, 33, 4389
- Griffin, D. C., Badnell, N. R., & Pindzola, M.S. 1998, *J. Phys. B*, 31, 3713
- Griffin, D. C., Badnell, N. R., Pindzola, M.S., & Shaw, J.A. 1999a, *J. Phys. B*, 32, 2139
- Griffin, D. C., Badnell, N. R., Pindzola, M.S., & Shaw, J.A. 1999b, *J. Phys. B*, 32, 4129
- Griffin, D. C., Badnell, N. R., & Pindzola, M.S. 2000, *J. Phys. B*, 33, 1013
- Heil, T. G., Green, S., & Dalgarno, A. 1982, *Phys. Rev. A*, 26, 3293
- Heil, T. G., Kirby, K., & Dalgarno, A. 1983, *Phys. Rev. A*, 27, 2826
- Hibbert, A. 1975, *Comput. Phys. Commun.*, 9, 141
- Hibbert, A., Biemont, E., Godefroid, M., & Vaeck, N. 1991, *A&AS*, 88, 505
- Huang, K.-N. 1984, *At. Data Nucl. Data Tables*, 30, 313
- Itoh, N., Sakamoto, T., & Kusano, S., 2000, *ApJS*, 128, 125

- Jordan, C., Sim, S. A., McMurry, A. D., & Aruvel, M. 2001, MNRAS, 326, 303
- Judge, P. G. 1998 ApJ, 500, 1009
- Jupen, C., & Engström, L. 1997, Phys. Scr., 56, 592
- Karzas, W. J., & Latter, R. 1961, ApJS, 6, 167
- Kastner, S. O. 1977, A&A, 54, 255
- Kastner, S. O. & Bhatia, A. K. 1979, A&A, 71, 211
- Keenan, F. P. 1988, Phys. Scr., 37, 57
- Keenan, F. P., Berrington, K. A., Burke, P. G., Dufton, P. L., & Kingston, A. E. 1986, Phys. Scr., 34, 216
- Keenan, F. P., McKenna, F. C., Bell, K. L., Ramsbottom, C. A., Wickstead, A. W., Aller, L. H., & Hyung, S. 1997, ApJ, 487, 457
- Keenan, F.P., et al. 2000, MNRAS, 315, 450
- Kelly, R. L. 1987, J. Phys. Chem. Ref. Data 16, Suppl. 1
- Kink, I., Jupen, C., Engström, L., Feldman, U., Laming, J. M., & Schühle, U. 1997, ApJ, 487, 956
- Kink, I., Engström, L., & Feldman, U. 1999, ApJ, 512, 496
- Kucera, T. A., Feldman, U., Widing, K. G., & Curdt, W. 2000, ApJ, 538, 424
- Landi, E. & Landini, M. 1998, A&AS, 133, 411
- Landi, E., & Landini, M. 2002, A&A, 384, 1124
- Landi, E., Landini, M., Dere, K. P., Young, P. R., & Mason, H. E. 1999, A&AS, 135, 339
- Landi, E., Doron, R., Feldman, U., & Doschek, G. A. 2001, ApJ, 556, 912
- Landi, E., Feldman, U., & Dere, K. P. 2002, ApJS, 139, 281
- Landman, D. A. 1973, Sol. Phys., 31, 81
- Landman, D. A. 1975, A&A, 43, 285
- Landman, D. A. 1978, ApJ, 220, 366
- Landman, D. A. 1980, ApJ, 240, 709
- Landman, D. A. & Brown, T. 1978, ApJ, 232, 636

- Lanzafame, A. C., Tully, J. A., Berrington, K. A., Dufton, P. L., & Byrne, P. B., 1993, MNRAS, 264, 402
- Lin, C. D., Johnson, W. R., & Dalgarno, A. 1977, Phys. Rev. A, 15, 154
- Louergue, M., Mason, H. E., Nussbaumer, H., & Storey, P. J. 1985, A&A, 150, 246
- Mason, H. E. 1975, MNRAS, 170, 651
- Mason, H.E., Doschek, G. A., Feldman, U., & Bhatia, A. K. 1979, A&A, 73, 74
- Mattioli, M., Fournier, K. B., Carraro, L., DeMichelis, C., Monier-Garbet, P., Puiatti, M. E., Sattin, F., Scarin, P., & Valisa, M. 1999, Phys. Rev. E, 60, 4760
- Mazzotta, P., Mazzitelli, G., Colafrancesco, S., & Vittorio, N. 1998, A&AS, 133, 403
- McLaughlin, B. M. & Bell, K. L. 2000, J. Phys. B, 33, 597
- Mendoza, C., & Zeippen, C.J. 1982, MNRAS, 198, 127
- Merkelis, G., Martinson, I., Kisielius, R., & Vilkas, M. J. 1999, Physica Scripta 59, 122
- Mewe, R., Lemen, J. R., & van den Oord G. H. J. 1986, A&AS, 65, 511
- Nahar, S. 1998, At. Data Nucl. Data Tables, 68, 183
- Nussbaumer, H., & Storey, P. J. 1978, A&A, 70, 37
- Pagano, I., Linsky, J. L., Carkner, L., Robinson, R. D., Woodgate, B., & Timothy, G. 2000, ApJ, 532, 497
- Parpia, F. A., & Johnson, W. R. 1982, Phys. Rev. A, 26, 1142.
- Penn, M. J., Arnaud, J., Mickey, D. L., & Labonte, B. J. 1994, ApJ, 436, 368
- Phillips, K. J. H., Bhatia, A. K., Mason, H. E., & Zarro, D. M. 1996, ApJ, 466, 549
- Phillips, K. J. H., Mewe, R., Harra-Murnion, L. K., Kaastra, J. S., Beiersdorfer, P., Brown, G. V., & Liedahl, D. A. 1999, A&A, 138, 381
- Raga, A. C., Velázquez, P. F., Cantó, J., Masciadri, E., & Rodríguez, L. F. 2001, ApJ, 559, L33
- Ramsbottom, C. A., & Bell, K. L. 1997, At. Data Nucl. Data Tables, 66, 65
- Ramsbottom, C. A., Bell, K. L., & Stafford, R. P., 1996, At. Data Nucl. Data Tables, 63, 57
- Ramsbottom, C. A., Bell, K. L., & Keenan, F. P. 1997, MNRAS, 284, 754
- Reader, J., & Sugar, J. 1975, J. Phys. Chem. Ref. Data, 4, 424

- Reid, R. H. G. 1988, *Adv. Atom. Mol. Phys.*, 25, 251
- Reid, R. H. G. & Schwarz, J. H. 1969, in *Proceedings 6th International Conference on Physics of Electronic and Atomic Collisions*, ed. I. Amdur (Cambridge: MIT), 236
- Ryans, R. S. I., Foster-Woods, V. J., Copeland F., Keenan, F. P., Matthews, A. & Reid, R. H. G. 1998, *At. Data Nucl. Data Tables*, 70, 179
- Ryans, R. S. I., Foster-Woods, V. J., & Keenan, F. P. 1999a, *ADNDT*, 73, 1
- Ryans, R. S. I., Foster-Woods, V. J., Reid, R. H. G., & Keenan, F. P. 1999b, *A&A*, 345, 663
- Rybicki, G. B., & Lightman, A. P. 1979, *Radiative Processes in Astrophysics* (New York: Wiley)
- Sampson, D. H., Zhang, H. L., & Fontes, C. J. 1991, *At. Data Nucl. Data Tables*, 48, 25
- Sawey, P. M. J., & Berrington, K. A. 1993, *At. Data Nucl. Data Tables*, 55, 81
- Seaton, M. J. 1987, *J. Phys. B*, 20, 6363
- Seaton, M. J., & Osterbrock, D. E. 1957, *ApJ*, 125, 66
- Seaton, M. J. 1964, *MNRAS*, 127, 191
- Shirai, T., Sugar, J., Musgrove, A., & Wiese, W.L. 2000, *J. Phys. Chem. Ref. Data, Monograph* 8
- Smith, R. K., Brickhouse, N. S., Liedahl, D. A., & Raymond, J. C. 2001, *ApJ*, 556, L91
- Stanghellini, L., & Kaler, J. B. 1989, *ApJ*, 343, 811
- Storey P. J., & Zeippen C. J. 2000, *MNRAS*, 312, 813
- Storey P. J., Mason, H. E., & Young, P. R. 2000, *A&AS*, 141, 285
- Sutherland, R. S. 1998, *MNRAS*, 300, 321
- Tayal, S. S. 1997, *ApJS*, 111, 459
- Tayal, S. S. 2000, *At. Data Nucl. Data Tables*, 76, 191
- Tayal, S. S. & Beatty, C. A. 1999, *Phys. Rev. A*, 59, 3622
- Verner, D. A., & Yakovlev, D. G. 1995, *A&AS*, 109, 125
- Wiese W. L., Smith M. W., & Glennon, B. M., *Atomic Transition Probabilities, Vol I, Hydrogen Through Neon*, NSRDS-NBS 4, 1966
- Young, P. R. & Mason, H. E. 1997, *Sol. Phys.*, 175, 523
- Young, P. R., Landi, E., & Thomas, R. J. 1998, *A&A*, 329, 291

- Young, P. R., Dupree, A. K., Wood, B. E., Redfield, S., Linsky, J. L., Ake, T. B., & Moos, H. W. 2001, *ApJ*, 555, L121
- Zeippen, C. J. 1987, *A&A*, 173, 410
- Zeippen, C. J., Butler, K., & Le Bourlot, J. 1987, *A&A*, 188, 251
- Zhang, H. L., & Pradhan, A. K. 1997, *A&A*, 123, 575
- Zhang, H. L., & Sampson, D. H. 1992, *At. Data Nucl. Data Tables*, 52, 143
- Zhang, H. L., & Sampson, D. H. 1997, *At. Data Nucl. Data Tables*, 65, 183
- Zhang, H. L., & Sampson, D. H. 1999, *At. Data Nucl. Data Tables*, 72, 153
- Zhang, H. L., & Sampson, D. H. 2001, *At. Data Nucl. Data Tables*, in preparation
- Zhang, H. L., Graziani, G., & Pradhan, A. K. 1994, *A&A*, 283, 319

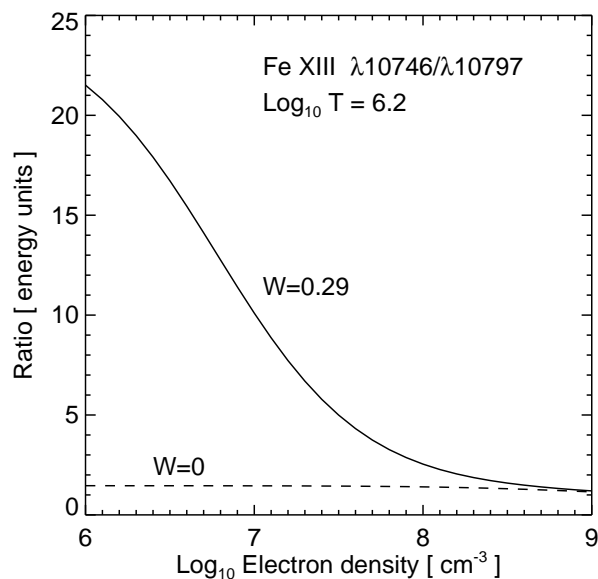


Fig. 3.— The Fe XIII $\lambda 10746/\lambda 10797$ ratio plotted as a function of density for two different dilution factors. $W = 0$ corresponds to no radiation field, while $W = 0.29$ corresponds to 0.1 source radii above the source surface ($r_* = 1.1$).

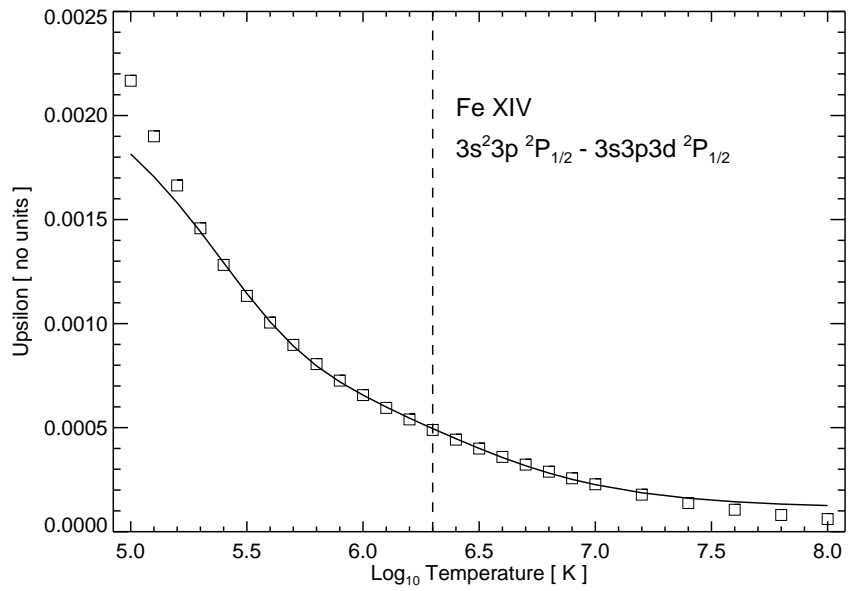


Fig. 4.— The squares show the Υ values for the Fe XIV $3s^23p\ ^2P_{1/2} - 3s3p3d\ ^2P_{1/2}$ transition, calculated by Storey et al. (2000). The solid line shows the values derived from the 5-point spline fit employed in CHIANTI, while the dashed line indicates the T_{\max} of the ion. At low and high temperatures the fit is seen to differ significantly from the original data, although good agreement is found for temperatures close to T_{\max} .

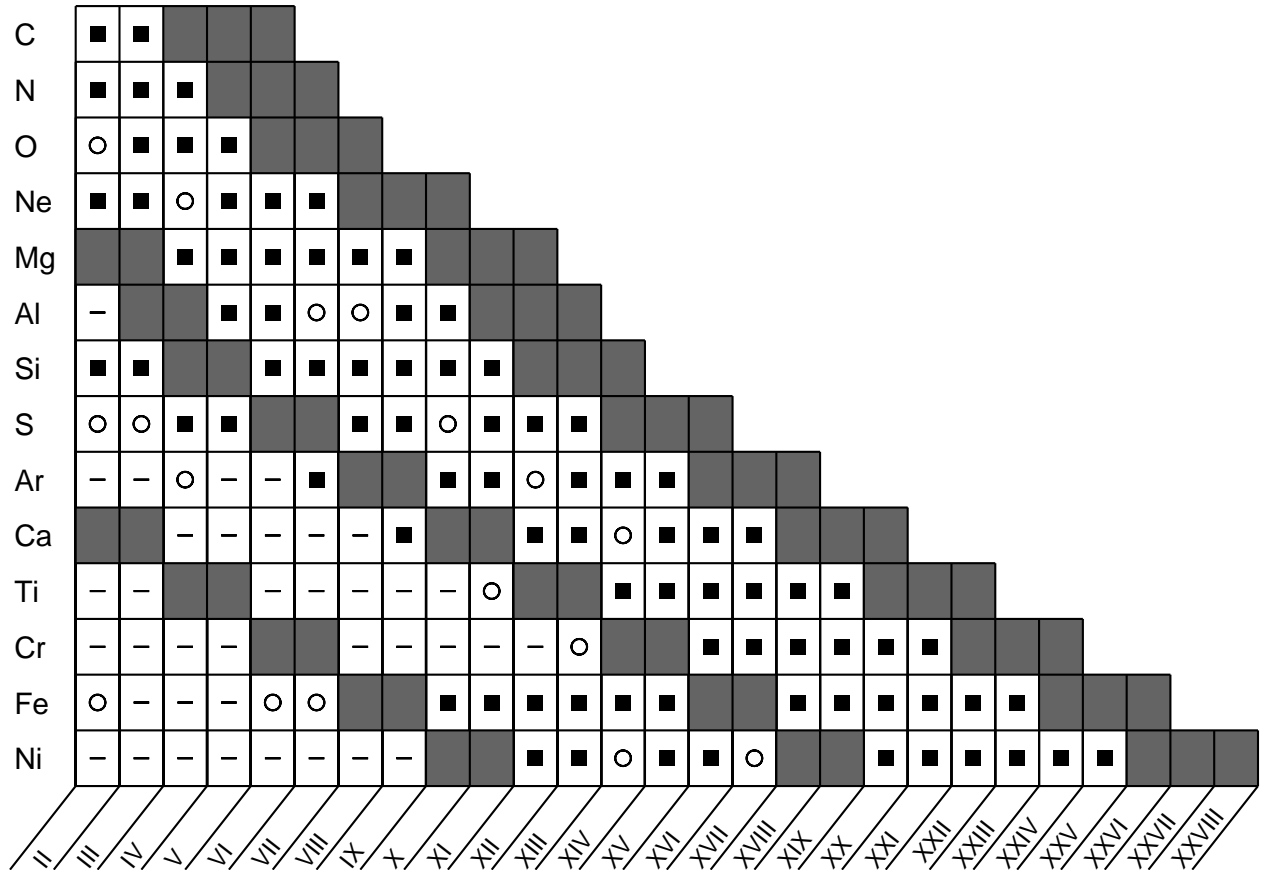


Fig. 5.— This figure indicates for which of the major elements in CHIANTI we have proton data. The shaded squares denote that proton rates are unimportant for these ions; small black squares denote ions for which data has been added to CHIANTI; circles indicate ions that are in CHIANTI but for which no proton data is available; and dashes indicate ions which are currently not in CHIANTI.

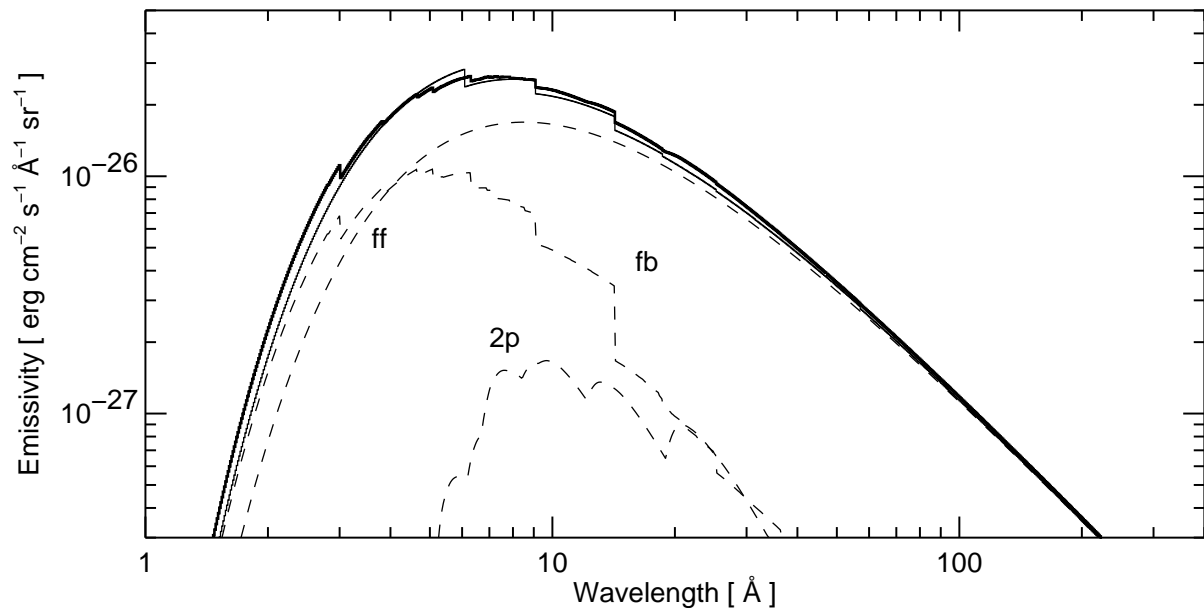


Fig. 6.— A comparison of the continuum emissivity predicted by CHIANTI (thick line) at a temperature of 1×10^7 K with that obtained through the analytic approximations of Mewe et al. (1986). The individual contributions of the CHIANTI free-free (ff), free-bound (fb) and two-photon (2p) continua are indicated with dashed lines.